Designation: E1457 – 15

Standard Test Method for Measurement of Creep Crack Growth Times in Metals[1]

This standard is issued under the fixed designation E1457; the number immediately following the designation indicates the year of original adoption or, in the case of revision, the year of last revision. A number in parentheses indicates the year of last reapproval. A superscript epsilon (ε) indicates an editorial change since the last revision or reapproval.

1. Scope

1.1 This test method covers the determination of creep crack initiation (CCI) and creep crack growth (CCG) in metals at elevated temperatures using pre-cracked specimens subjected to static or quasi-static loading conditions. The solutions presented in this test method are validated for base material (i.e. homogenous properties) and mixed base/weld material with inhomogeneous microstructures and creep properties. The CCI time, $t_{0.2}$, which is the time required to reach an initial crack extension of $\delta a_i = 0.2$ mm to occur from the onset of first applied force, and CCG rate, $\dot{a}$ or da/dt are expressed in terms of the magnitude of creep crack growth correlated by fracture mechanics parameters, C^* or K, with C^* defined as the steady state determination of the crack tip stresses derived in principal from $C^*(t)$ and C_t (**1-17**).[2] The crack growth derived in this manner is identified as a material property which can be used in modeling and life assessment methods (**17-28**).

1.1.1 The choice of the crack growth correlating parameter C^*, $C^*(t)$, C_t, or K depends on the material creep properties, geometry and size of the specimen. Two types of material behavior are generally observed during creep crack growth tests; creep-ductile (**1-17**) and creep-brittle (**29-44**). In creep ductile materials, where creep strains dominate and creep crack growth is accompanied by substantial time-dependent creep strains at the crack tip, the crack growth rate is correlated by the steady state definitions of C_t or $C^*(t)$, defined as C^* (see 1.1.4). In creep-brittle materials, creep crack growth occurs at low creep ductility. Consequently, the time-dependent creep strains are comparable to or dominated by accompanying elastic strains local to the crack tip. Under such steady state creep-brittle conditions, C_t or K could be chosen as the correlating parameter (**8-14**).

1.1.2 In any one test, two regions of crack growth behavior may be present (**12, 13**). The initial transient region where elastic strains dominate and creep damage develops and in the steady state region where crack grows proportionally to time. Steady-state creep crack growth rate behavior is covered by this standard. In addition specific recommendations are made in 11.7 as to how the transient region should be treated in terms of an initial crack growth period. During steady state, a unique correlation exists between da/dt and the appropriate crack growth rate relating parameter.

1.1.3 In creep ductile materials, extensive creep occurs when the entire un-cracked ligament undergoes creep deformation. Such conditions are distinct from the conditions of small-scale creep and transition creep (**1-10**). In the case of extensive creep, the region dominated by creep deformation is significant in size in comparison to both the crack length and the uncracked ligament sizes. In small-scale-creep only a small region of the un-cracked ligament local to the crack tip experiences creep deformation.

1.1.4 The creep crack growth rate in the extensive creep region is correlated by the $C^*(t)$-integral. The C_t parameter correlates the creep crack growth rate in the small-scale creep and the transition creep regions and reduces, by definition, to $C^*(t)$ in the extensive creep region (**5**). Hence in this document the definition C^* is used as the relevant parameter in the steady state extensive creep regime whereas $C^*(t)$ and/or C_t are the parameters which describe the instantaneous stress state from the small scale creep, transient and the steady state regimes in creep. The recommended functions to derive C^* for the different geometries shown in Annex A1 is described in Annex A2.

1.1.5 An engineering definition of an initial crack extension size δa_i is used in order to quantify the initial period of crack development. This distance is given as 0.2 mm. It has been shown (**41-44**) that this initial period which exists at the start of the test could be a substantial period of the test time. During this early period the crack tip undergoes damage development as well as redistribution of stresses prior reaching steady state. Recommendation is made to correlate this initial crack growth period defined as $t_{0.2}$ at $\delta a_i = 0.2$ mm with the steady state C^* when the crack tip is under extensive creep and with K for creep brittle conditions. The values for C^* and K should be calculated at the final specified crack size defined as $a_o + \delta a_i$ where a_o is initial size of the starter crack.

1.1.6 The recommended specimens for CCI and CCG testing is the standard compact tension specimen C(T) (see Fig. A1.1) which is pin-loaded in tension under constant loading conditions. The clevis setup is shown in Fig. A1.2 (see 7.2.1 for

[1] This test method is under the jurisdiction of ASTM Committee E08 on Fatigue and Fracture and is the direct responsibility of Subcommittee E08.06 on Crack Growth Behavior.

Current edition approved June 1, 2015. Published October 2015. Originally approved in 1992. Last previous edition approved in 2000 as E1457 – 07$^{\varepsilon 4}$. DOI: 10.1520/E1457-15.

[2] The boldface numbers in parentheses refer to the list of references at the end of this standard.

details). Additional geometries which are valid for testing in this procedure are shown in Fig. A1.3. These are the C-ring in tension CS(T), middle crack specimen in tension M(T), single edge notched tension SEN(T), single edge notched bend SEN(B), and double edge notched tension DEN(T). In Fig. A1.3, the specimens' side-grooving-position for measuring displacement at the force-line displacement (FLD) and crack mouth opening displacement (CMOD) and also positions for the potential drop (PD) input and output leads are shown. Recommended loading for the tension specimens is pin-loading. The configurations, size range are given in Table A1.1 of Annex A1, (**43-47**). Specimen selection will be discussed in 5.9.

1.1.7 The state-of-stress at the crack tip may have an influence on the creep crack growth behavior and can cause crack-front tunneling in plane-sided specimens. Specimen size, geometry, crack length, test duration and creep properties will affect the state-of-stress at the crack tip and are important factors in determining crack growth rate. A recommended size range of test specimens and their side-grooving are given in Table A1.1 in Annex A1. It has been shown that for this range the cracking rates do not vary for a range of materials and loading conditions (**43-47**). Suggesting that the level of constraint, for the relatively short term test durations (less than one year), does not vary within the range of normal data scatter observed in tests of these geometries. However it is recommended that, within the limitations imposed on the laboratory, that tests are performed on different geometries, specimen size, dimensions and crack size starters. In all cases a comparison of the data from the above should be made by testing the standard *C(T)* specimen where possible. It is clear that increased confidence in the materials crack growth data can be produced by testing a wider range of specimen types and conditions as described above.

1.1.8 Material inhomogeneity, residual stresses and material degradation at temperature, specimen geometry and low-force long duration tests (mainly greater that one year) can influence the rate of crack initiation and growth properties (**42-50**). In cases where residual stresses exist, the effect can be significant when test specimens are taken from material that characteristically embodies residual stress fields or the damaged material, or both. For example weldments, or thick cast, forged, extruded, components, plastically bent components and complex component shapes, or a combination thereof, where full stress relief is impractical. Specimens taken from such component that contain residual stresses may likewise contain residual stresses which may have altered in their extent and distribution due to specimen fabrication. Extraction of specimens in itself partially relieves and redistributes the residual stress pattern; however, the remaining magnitude could still cause significant effects in the ensuing test unless post-weld heat treatment (PWHT) is performed. Otherwise residual stresses are superimposed on applied stress and results in crack-tip stress intensity that is different from that based solely on externally applied forces or displacements. Not taking the tensile residual stress effect into account will produce C^* values lower than expected effectively producing a faster cracking rate with respect to a constant C^*. This would produce conservative estimates for life assessment and non-conservative calculations for design purposes. It should also be noted that distortion during specimen machining can also indicate the presence of residual stresses.

1.1.9 Stress relaxation of the residual stresses due to creep and crack extension should also be taken into consideration. No specific allowance is included in this standard for dealing with these variations. However the method of calculating C^* presented in this document which used the specimen's creep displacement rate to estimate C^* inherently takes into account the effects described above as reflected by the instantaneous creep strains that have been measured. However extra caution should still be observed with the analysis of these types of tests as the correlating parameters K and C^* shown in Annex A2 even though it is expected that stress relaxation at high temperatures could in part negate the effects due to residual stresses. Annex A4 presents the correct calculations needed to derive J and C^* for weldment tests where a mis-match factor needs to be taken into account.

1.1.10 Specimen configurations and sizes other than those listed in Table A1.1 which are tested under constant force will involve further validity requirements. This is done by comparing data from recommended test configurations. Nevertheless, use of other geometries are applicable by this method provided data are compared to data obtained from standard specimens (as identified in Table A1.1) and the appropriate correlating parameters have been validated.

1.2 The values stated in SI units are to be regarded as the standard. The inch-pound units given in parentheses are for information only.

1.3 *This standard does not purport to address all of the safety concerns, if any, associated with its use. It is the responsibility of the user of this standard to establish appropriate safety and health practices and determine the applicability of regulatory limitations prior to use.*

2. Scope of Material Properties Data Resulting from This Standard

2.1 This test method covers the determination of initial creep crack extension (CCI) times and growth (CCG) in metals at elevated temperature using pre-cracked specimens subjected to static or quasi-static loading conditions. The metallic materials investigated range from creep-ductile to creep-brittle conditions.

2.2 The crack growth rate $\dot{a}$ or da/dt is expressed in terms of the magnitude of CCG rate relating parameters, $C^*(t)$, C_t or K. The resulting output derived as $\dot{a}vC^*$ (as the steady state formulation of $C^*(t)$), or C_t for creep-ductile materials or as $\dot{a}vK$ (for creep-brittle materials) is deemed as material property for CCG.

2.3 In addition for CCI derivation of crack extension time $t_{0.2}$ v C^* (for creep-ductile materials) or $t_{0.2}vK$ (for creep-brittle materials) can also be used as a material property for the purpose of modeling and remaining life assessment.

2.4 The output from these results can be used as 'Benchmark' material properties data which can subsequently be used

in crack growth numerical modeling, in component design and remaining life assessment methods.

3. Referenced Documents

3.1 *ASTM Standards:*[3]

E4 Practices for Force Verification of Testing Machines
E74 Practice of Calibration of Force-Measuring Instruments for Verifying the Force Indication of Testing Machines
E83 Practice for Verification and Classification of Extensometer Systems
E139 Test Methods for Conducting Creep, Creep-Rupture, and Stress-Rupture Tests of Metallic Materials
E220 Test Method for Calibration of Thermocouples By Comparison Techniques
E399 Test Method for Linear-Elastic Plane-Strain Fracture Toughness K_{Ic} of Metallic Materials
E647 Test Method for Measurement of Fatigue Crack Growth Rates
E813 Test Method for JIc, A Measure of Fracture Toughness
E1152 Test Method for Determining-J-R-Curves
E1820 Test Method for Measurement of Fracture Toughness
E1823 Terminology Relating to Fatigue and Fracture Testing
E2818 Practice for Determination of Quasistatic Fracture Toughness of Welds

4. Terminology

4.1 Terminology related to fracture testing contained in Terminology E1823 is applicable to this test method. Additional terminology specific to this standard is detailed in 4.2 and 4.3. For clarity and easier access within this document some of the terminology in E1823 relevant to this standard is repeated below (see Terminology E1823, for further discussion and details).

4.2 *Definitions:*

4.2.1 *creep crack growth (CCG) rate, da/dt, Δa/Δat [L/t]*—the rate of crack extension caused by creep damage and expressed in terms of average crack extension per unit time. **[E1823]**

4.2.2 *C*(t)-integral, C*(t) [$FL^{-1}T^{-1}$]*—a mathematical expression a line or surface integral that encloses the crack front from one crack surface to the other, used to characterize the local stress-strain rate fields at any instant around the crack front in a body subjected to extensive creep conditions

4.2.2.1 *Discussion*—The parameter relevant to creep crack growth is given as the *C*(t)*-Integral consisting of a line or surface integral that encloses the crack front from one crack surface to the other. *C*(t)* is used to characterize the local stressstrain rate fields at any instant around the crack front in a body subjected to extensive creep conditions.

4.2.2.2 *Discussion*—The *C*(t)* expression for a two-dimensional crack, in the *x-z* plane with the crack front parallel to the *z*-axis, is the line integral:

$$C^* = \int_{\Gamma} \left(\dot{W} dy - T_i \frac{\partial \dot{u}_i}{\partial x} ds \right) \quad (1)$$

where:

$\dot{W}$ = instantaneous stress-power or energy rate per unit volume,
Γ = path of the integral, that encloses (that is, contains) the crack tip contour,
ds = increment in the contour path,
T = outward traction vector on ds,
$\dot{u}$ = displacement rate vector at ds,
x, y, z = rectangular coordinate system, and

$T_i \frac{\partial \dot{u}_i}{\partial x}$ is the rate of stress-power input into the area enclosed by Γ across the elemental length ds.

4.2.2.3 *Discussion*—The value of *C*(t)* from this equation is path-independent for materials that deform according to constitutive law that may be separated into single-value time and stress functions or strain and stress functions of the forms:

$$\dot{\varepsilon} = f_1(t) f_2(\sigma) \quad (2)$$

$$\dot{\varepsilon} = f_3(\varepsilon) f_4(\sigma) \quad (3)$$

where f_1-f_4 represent functions of elapsed time, t, strain, ε and applied stress, σ, respectively and $\dot{\varepsilon}$ is the strain rate.

4.2.2.4 *Discussion*—For materials exhibiting creep deformation for which the above equation is path-independent, the *C*(t)*-integral is equal to the value obtained from two, stressed, identical bodies with infinitesimally differing crack areas. This value is the difference in the stress-power per unit difference in crack area at a fixed value of time and displacement rate, or at a fixed value of time and applied force.

4.2.2.5 *Discussion*—The value of *C*(t)* corresponding to the steady-state conditions is called *C**. Steady-state is said to have been achieved when a fully developed creep stress distribution has been produced around the crack tip. This occurs when the secondary creep deformation characterized by the following equation dominates the behavior of the specimen.

$$\dot{\varepsilon}_{ss} = A\sigma^{n} \quad (4)$$

4.2.2.6 *Discussion*—This steady state in *C** does not necessarily mean steady state crack growth rate. The latter occurs when steady state damage develops at the crack tip. In this test method, this behavior is observed as 'tails' at the early stages of crack growth. This standard deals with this region as the initial crack extension period defined as time, $t_{0.2}$, measured for an initial crack growth of 0.2 mm after first loading (see 11.8.8 for further details).

4.2.3 *C_t parameter, C_t [$FL^{-1}T^{-1}$]*—a parameter equal to the value obtained from two identical bodies with infinitesimally differing crack areas, each subjected to stress, as the difference in stress-power per unit difference in crack area at a fixed value of time and displacement rate, or at a fixed value of time applied force for an arbitrary constitutive law.

4.2.3.1 *Discussion*—The value of C_t is path-independent and is identical to *C*(t)* for extensive creep conditions when the constitutive law described in 4.2.2 applies.

4.2.3.2 *Discussion*—Under small-scale creep conditions, *C*(t)* is not path-independent and is related to the crack tip

[3] For referenced ASTM standards, visit the ASTM website, www.astm.org, or contact ASTM Customer Service at service@astm.org. For *Annual Book of ASTM Standards* volume information, refer to the standard's Document Summary page on the ASTM website.

stress and strain fields only for paths local to the crack tip and well within the creep zone boundary. Under these circumstances, C_t is related uniquely to the rate of expansion of the creep zone size (**13-15**). There is considerable experimental evidence that the C_t parameter (**5, 11, 13**) which extends the *C*(t)-integral* concept into small-scale and the transition creep regime, correlates uniquely with creep crack growth rate in the entire regime ranging from small-scale to extensive creep regime.

4.2.3.3 *Discussion*—For a specimen with a crack subject to constant force, *P*:

$$C_t = \frac{P\dot{V}_c}{BW}(f'/f)$$

and

$$f' = \frac{df}{d(a/W)}$$

4.2.4 *force-line displacement due to creep, elastic and plastic strain, V [L]*—the total displacement measured at the loading pins (V^{FLD}) due to the force placed on the specimen at any instant and the subsequent crack extension that is associated with the accumulation of creep, elastic and plastic strains in the specimen.

4.2.4.1 *Discussion*—In creeping bodies, the total displacement at the force-line V^{FLD} can be partitioned into an instantaneous elastic part V_e, a plastic part, V_p, and a time-dependent creep part V_c where:

$$V = V_e + V_p + V_c \quad (5)$$

The corresponding symbols for the rates of force-line displacement components shown in Eq 5 are given respectively as $\dot{V}$, $\dot{V}_e$, $\dot{V}_p$, $\dot{V}_c$. This information is used to derive the parameter C^* and C_t. See Section 11.

4.2.4.2 *Discussion*—For the set of specimens in Annex A1, Table A1.1 for creep ductile material where creep strains dominate and in which test times are longer (usually >1000 hours), the elastic and plastic displacement rate components are small compared to the creep and therefore it is recommended to use the total displacement rate $\dot{V}$ assuming that $\dot{V}_c \approx \dot{V}$ to derive the steady state C^*. See Section 11 for detailed discussion.

4.2.4.3 *Discussion*—The force-line displacement associated with just the creep strains is expressed as V_c.

4.2.5 *J-integral, J [FL^{-1}]*—a mathematical expression, a line or surface integral that encloses the crack front from one crack surface to the other, used to characterize the local stress-strain field around the crack front.

4.2.6 *net thickness, B_N [L]*—distance between the roots of the side grooves in side-grooved specimens.

4.2.7 *original crack size, a_o [L]* —the physical crack size at the start of testing.

4.2.8 *specimen thickness, B [L]*—distance between the parallel sides of a test specimen.

4.2.9 *specimen width, W [L]*—the distance from a reference position (for example, the front edge of a bend specimen or the force line of a compact specimen) to the rear surface of the specimen.

4.2.10 *stress intensity factor, K [FL$^{-3/2}$]*—the magnitude of the mathematically ideal crack tip stress field (a stress-field singularity) for Mode 1 in a homogeneous, linear-elastic body.

4.2.11 *transition time, t_T [T]*—time required for extensive creep conditions to develop in a cracked body under sustained loading. For specimens, this is typically the time required for the creep deformation zone to spread through a substantial portion of the uncracked ligament, or in the region that is under the influence of a crack in the case of a finite crack in a semi-infinite medium. This limit is employed to validate the steady state correlating parameter C^*. An estimate of transition time for materials that creep according to the power-law can be obtained from the following equation:

$$t_T = \frac{K^2(1 - \nu^2)}{E(n + 1)\, C^*}$$

where:

ν = Poisson's ratio, and
n = secondary creep exponent.

4.2.12 *yield strength, σ_{YS} [FL^{-2}]*—the stress at which the material exhibits a deviation equal to a strain of 0.02 % offset from the proportionality of stress to strain.

4.3 *Definitions of Terms Specific to This Standard:*

4.3.1 *creep zone boundary* —the locus of points ahead of the crack front where the equivalent strain caused by the creep deformation equals 0.002 (0.2 %) (**16**).

4.3.1.1 *Discussion*—Under small-scale creep conditions, the creep zone expansion with time occurs in a self-similar manner for planar bodies, (**10**) thus, the creep zone size, r_c, can be defined as the distance to the creep zone boundary from the crack tip at a fixed angle, θ, with respect to the crack plane. The rate of expansion of the creep zone size is designated as $\dot{r}_c$ (θ).

4.3.2 *crack-plane orientation*—an identification of the plane and direction of fracture or crack extension in relation to product configuration. This identification is designated by a hyphenated code with the first letter(s) representing the direction normal to the crack plane and the second letter(s) designating the expected direction of crack propagation.

4.3.3 *crack size, a [L]*—in this test method, the physical crack size is represented as a_p. The subscript, *p*, is everywhere implied (see Terminology E1823). a_o is defined as the initial crack size.

4.3.4 *initial crack extension increment (CCI) after full force-up, δa_i [L]*—the recommended time taken to crack extension of δa_i = 0.2 mm after first application of force for defining a crack growth period $t_{0.2}$ in hours as a function of $C^*(t)$, C_t, or K value taken. at crack length $a_o + \delta a_i$.

4.3.5 *initial crack time to 0.2 mm, $t_{0.2}$ [T]*—the time to δa_i = 0.2 mm (0.008 in.) of crack extension δ *a* by creep after full loading. This size is chosen as the limit of accuracy set for crack extension measurements in laboratory geometries.

5. Summary of Test Method

5.1 The main objective of creep crack growth testing is the determination of the relationship between the time and rate of crack growth, *da/dt*, due to creep and the applied value of the appropriate crack growth rate relating parameter. In addition

results for time to crack extension of 0.2 mm at force-up (CCI) as defined in 1.1.5 are also correlated from the experimental data. This test method involves loading of sharply notched by means of EDM or fatigue pre-cracked specimens (see 8.8), using the recommended geometries, heated to the test temperature by means of a suitable furnace. The applied force is either held constant with time or is changed slowly enough to be considered quasi-static. The temperature must be constantly monitored to ensure that it remains at the specified level within allowable limits during the test. If servo-mechanical loading systems are used to maintain constant force, or if tests are conducted under conditions other than constant force, a record of force versus time also must be maintained.

5.2 Three different loading methods are available for creep crack growth testing. Dead weight loading is the recommended method and is the most commonly used method for loading specimens. In addition, constant displacement (**29**) and constant displacement rate (**1-4, 39**) loading may also be used but are only recommended when working with extremely brittle materials. For tests conducted under conditions other than dead-weight loading, the user must compare the results and verify the analysis from tests performed under dead-weight loading conditions.

5.3 It is recommended to carry out long term tests (at least >1000 h and usually, if possible, between 5000 to 10 000 h) in order to reduce crack tip plasticity which would occur at higher forces and allow for steady state creep cracking to take place. Large forces should be avoided since this will induce either fast fracture or extensive deformation due to creep or plastic collapse and/or rupture, thus rendering the crack growth test as void. Data from fast test are usually not appropriate for life assessment purposes as they may not reflect the stress state of the component at the crack-tip.

5.4 The crack size and force-line displacements are continuously recorded, digitally or autographically on strip-chart recorders, as a function of time. The force, force-line displacement and crack size data are numerically processed as discussed later to obtain the crack growth rate versus $C^*(t)$, C_t or K relationship.

5.5 Data scatter that is usually present in creep crack growth experiments (**43, 45, 51, 52**). This will indicate that more than one test should be performed to gain confidence in the results. The number of specimens to be tested is dependent on a number of factors (**52**) such as the number of test variables (specimen type, size, dimension, crack size, force, CCI and CCG range and material batches) being considered. In general it is recommended for the range of conditions that a minimum of five tests at different forces should be performed to produce overlapping crack growth data over the region of CCG rate of interest. Additional repeat tests would be preferable, but not compulsory, to improve confidence in the derived data range.

5.6 If the material exhibits such factors as irregular grain sizes and voids, weld (X-weld, HAZ) and other inhomogeneity the minimum number of tests should be increased (see 5.5). Also, more tests should be performed if the material creep crack growth behavior exhibits increased scatter regardless of the reason for the variability. If there is insufficient material available or if there are other reasons which would restrict multiple testing then the results should be considered with increased caution.

5.7 In some cases crack growth information is needed for the initial start of the test where steady state cracking has not been reached. Also this period coincides with the limit of accuracy in crack growth measurement (recommended as 0.2 mm see 1.1.2 (**35**). The data produced for (CCI) will therefore be one point per test (similar to uniaxial rupture tests). Hence more tests would be needed to accommodate the variability in the results. The minimum number of tests recommended will depend on the level of scatter, but should not be less than 5 tests which should also uniformly cover test times of interest.

5.8 *Specimen Selection*—For all cases attention must be given to the proper selection of specimen. The C(T) is always the primary choice as there is ample reference in the literature to the testing and analysis of this geometry.

5.9 The choice of specimen should reflect a number of factors. These priorities can be listed as follows:

5.9.1 Availability and the size of material prepared for testing indicates the number of specimens that can be tested.

5.9.2 Material creep ductility and stress sensitivity; for creep brittle specimens the C(T) is recommended.

5.9.3 Capacity of the test rig; the 3-point bend specimens and the C(T) specimens will typically take lower forces.

5.9.4 Type of loading (tension, bending, tension/bending) should be taken into consideration.

5.9.5 Compatibility with size and stress state of the specimen with the component under investigation.

5.9.6 Following a test if the crack front is substantially leading in the centre the indications are that constraint should be increased. If the crack front is substantially receding at the centre the opposite applies-This can be remedied by changing the size, thickness, side-grooving or the geometry of the specimen used for testing. See 8.3.

5.9.7 The length of time and temperature of testing; this will dictate the size, the applied force, initial crack size and side-grooving of the specimen.

5.9.8 *Discussion*—It is unlikely that all conditions for material selection can be satisfied at any one time. The main priority is to produce a test environment for stable crack growth to occur under steady state conditions. Therefore compromises may need to be made. This document goes part of the way to assist the user in this choice by identifying specific detail of a number of geometries. The appropriate decision may, however, need expert advice in the relevant field or industry.

6. Significance and Use

6.1 Creep crack growth rate expressed as a function of the steady state C^* or K characterizes the resistance of a material to crack growth under conditions of extensive creep deformation or under brittle creep conditions. Background information on the rationale for employing the fracture mechanics approach in the analyses of creep crack growth data is given in (**11, 13, 30-35**).

6.2 Aggressive environments at high temperatures can significantly affect the creep crack growth behavior. Attention must be given to the proper selection and control of temperature and environment in research studies and in generation of design data.

6.2.1 Expressing CCI time, $t_{0.2}$ and CCG rate, *da/dt* as a function of an appropriate fracture mechanics related parameter generally provides results that are independent of specimen size and planar geometry for the same stress state at the crack tip for the range of geometries and sizes presented in this document (see Annex A1). Thus, the appropriate correlation will enable exchange and comparison of data obtained from a variety of specimen configurations and loading conditions. Moreover, this feature enables creep crack growth data to be utilized in the design and evaluation of engineering structures operated at elevated temperatures where creep deformation is a concern. The concept of similitude is assumed, implying that cracks of differing sizes subjected to the same nominal $C^*(t)$, C_t, or K will advance by equal increments of crack extension per unit time, provided the conditions for the validity for the specific crack growth rate relating parameter are met. See 11.7 for details.

6.2.2 The effects of crack tip constraint arising from variations in specimen size, geometry and material ductility can influence $t_{0.2}$ and *da/dt*. For example, crack growth rates at the same value of $C^*(t)$, C_t in creep-ductile materials generally increases with increasing thickness. It is therefore necessary to keep the component dimensions in mind when selecting specimen thickness, geometry and size for laboratory testing.

6.2.3 Different geometries as mentioned in 1.1.6 may have different size requirements for obtaining geometry and size independent creep crack growth rate data. It is therefore necessary to account for these factors when comparing *da/dt* data for different geometries or when predicting component life using laboratory data. For these reasons, the scope of this standard is restricted to the use of specimens shown in Annex A1 and the validation criteria for these specimens are specified in 11.2.3 and 11.7. However if specimens other than the C(T) geometry are used for generating creep crack growth data, then the *da/dt* data obtained should, if possible, be compared against test data derived from the standard C(T) tests in order to validate the data.

6.2.4 Creep cracks have been observed to grow at different rates at the beginning of tests compared with the rates at equivalent $C^*(t)$, C_t or K values for cracks that have sustained previous creep crack extension (**12, 13**). This region is identified as 'tail'. The duration of this transient condition, 'tail', varies with material and initially applied force level. These transients are due to rapid changes in the crack tip stress fields after initial elastic loading and/or due to an initial period during which a creep damage zone evolves at the crack tip and propagates in a self-similar fashion with further crack extension (**12, 13**). This region is separated from the steady-state crack extension which follows this period and is characterized by a unique *da/dt* versus $C^*(t)$, C_t or K relationship. This transient region, especially in creep-brittle materials, can be present for a substantial fraction of the overall life (**35**). Criteria are provided in this standard to quantify this region as an initial crack growth period (see 1.1.5) and to use it in parallel with the steady state crack growth rate data. See 11.8.8 for further details.

6.3 Results from this test method can be used as follows:

6.3.1 Establish predictive models for crack incubation periods and growth using analytical and numerical techniques (**18-21**).

6.3.2 Establish the influence of creep crack development and growth on remaining component life under conditions of sustained loading at elevated temperatures wherein creeps deformation might occur (**23-28**).

NOTE 1—For such cases, the experimental data must be generated under representative loading and stress-state conditions and combined with appropriate fracture or plastic collapse criterion, defect characterization data, and stress analysis information.

6.3.3 Establish material selection criteria and inspection requirements for damage tolerant applications.

6.3.4 Establish, in quantitative terms, the individual and combined effects of metallurgical, fabrication, operating temperature, and loading variables on creep crack growth life.

6.4 The results obtained from this test method are designed for crack dominant regimes of creep failure and should not be applied to cracks in structures with wide-spread creep damage which effectively reduces the crack extension to a collective damage region. Localized damage in a small zone around the crack tip is permissible, but not in a zone that is comparable in size to the crack size or the remaining ligament size. Creep damage for the purposes here is defined by the presence of grain boundary cavitation. Creep crack growth is defined primarily by the growth of intergranular time-dependent cracks. Crack tip branching and deviation of the crack growth directions can occur if the wrong choice of specimen size, side-grooving and geometry is made (see 8.3). The criteria for geometry selection are discussed in 5.8.

7. Apparatus

7.1 *Testing Machine*—This standard does not recommend a specific type of testing equipment. It does however specify accuracy limits for the test equipment and suggestions for the types of equipment that could be used to achieve the accuracy limits specified.

7.1.1 Dead-weight or servo-mechanical loading machines capable of maintaining a constant force or maintaining constant displacement rates in the range of 10^{-5} to 1 mm/h can be used for creep crack growth testing. If servo-hydraulic machines are used under constant force conditions, the force must be monitored continuously and the variations in the indicated force must not exceed ±1.0 % of the nominal value at any time during the test. If either constant displacement rate or constant displacement is used, the indicated displacement must be within 1 % of the nominal value at any given time during the test.

7.1.2 The accuracy of the testing machine shall be within the permissible variation specified in Practice E4.

7.1.3 If lever-type, dead-weight creep machines are used, it is preferable that they automatically maintain the lever arm in a horizontal position. If such a device is not available, the lever arm should be manually adjusted at such intervals so that the

arm position at any time does not deviate from the horizontal by an amount leading to 1 %, variation of force on the specimen.

7.1.4 Precautions should be taken to ensure that the force on the specimen is applied as nearly axial as possible.

7.2 *Grips and Fixtures* for specimens listed in Annex A1: It is allowed to deviate from the recommended testing apparatus as long as the relevant accuracies and loading conditions are adhered to.

7.2.1 Clevis assemblies shall be incorporated in the force train at both the top and bottom of the specimen to allow in-plane rotation as the specimen is loaded. Fig. A1.2 shows an example for the clevis setup for the tension specimens shown in Fig. A1.3. The bend specimen will be simply a 3-point bend loading assembly.

7.2.2 Suggested proportions and critical tolerances of the fixtures shall be within the specified variation shown in Fig. A1.2. Note that surface finish does not have a major effect on creep crack growth and therefore a normal smooth finish to the specimen is sufficient.

7.2.3 The pin-to-hole clearances are designed to minimize friction thereby eliminating unacceptable end-movements that would invalidate the specimen calibrations for determining K, J, and $C^*(t)$.

7.2.4 The material for the grips and pull rods should be chosen with due regard to test temperature and force level to be employed. Some elevated temperature materials currently being used include American Iron and Steel Institute (AISI) Grade 304 and 316 stainless steel, Grade A286 steel, nickel-based superalloys like alloy 718 or alloy X750. The loading pins are machined from A286 steel (or equivalent or better temperature resistant steel) and are heat treated such that they develop a high resistance to creep deformation and rupture.

7.3 *Alignment of Grips*—It is important that attention be given to achieving good alignment in the force-line through careful machining of all gripping fixtures. The length of the force train should be chosen with proper attention to the height of the furnace for heating the test specimen.

7.4 *Heating Apparatus:*

7.4.1 The apparatus for, and method of, heating the specimens should provide the temperature control necessary to satisfy the requirements in 10.3, without manual adjustments more frequent than once in each 24-h period after force application.

7.4.2 Heating shall be by an electric resistance or radiation furnace with the specimen in air at atmospheric pressure unless other media are specifically agreed upon in advance.

NOTE 2—The test conditions in which tests are performed may have a considerable effect on the results. This is particularly true when properties are influenced by plasticity, environmental effects, oxidation or other types of corrosion.

7.5 *Temperature-Measurement Apparatus*—The method of temperature measurement must be sufficiently sensitive and reliable to ensure that the specimen temperature is within the limits specified in 10.3. For details of types of apparatus used see Specification E139.

7.6 *Displacement Gage*—For the measurement of the *FLD* or *CMOD* displacement during the test.

7.6.1 Continuous displacement measurement is needed to evaluate the magnitude of $C^*(t)$ and C_t at any time during the test. Displacement measurements must be made on the force-line.

7.6.2 As a guide, the displacement gage should have a working range no more than twice the displacement expected during the test. Accuracy of the gage should be within ±1 % of the full working range of the gage. In calibration, the maximum deviation of the individual data points from the fit to the data shall not exceed ±1 % of the working range.

7.6.3 Knife edges are recommended for friction-free seating of the gage. Parallel alignment of the knife edges must be maintained to within ±1°.

7.6.4 The displacement along the force-line may be directly measured by attaching the entire clip gage assembly to the specimen and placing the whole assembly in the furnace. Alternatively, the displacements can be transferred outside the furnace with a rod and tube assembly such as that shown in Figs. A1.4 and A1.5.

7.6.5 In the latter procedure, the transducer is placed outside the furnace. It is important to make the tube and rod from materials that are thermally stable and are from the same material to avoid erroneous readings caused by differences in thermal expansion coefficients. Other designs that can measure displacements to the same levels of accuracy may also be used.

7.7 *Apparatus for Crack Size Measurement*—A crack size monitoring technique capable of reliably resolving crack extensions of at least ±0.1 mm at test temperature is recommended for creep crack growth measurements. Since crack extension across the thickness of the specimen is not always uniform, surface crack size measurements by optical means are not considered reliable as a primary method. Optical observation may be used as an auxiliary measurement method. The selected crack size measurement technique must be capable of measuring the average crack size across the thickness. The most commonly used technique for crack size measurement during creep crack growth testing is the electric potential technique that is described in Annex A4.

NOTE 3—The crack size measurement precision is herein defined as the standard deviation of the mean value of crack size determined for a set of replicate measurements.

7.8 *Room Temperature Control*—The ambient temperature in the room should be sufficiently constant so that the specimen temperature variations do not exceed the limits stated in 10.3.5.

7.9 *Timing Apparatus*—Suitable means for recording and measuring elapsed time to within 1 % of the elapsed time should be provided.

8. Specimen Configuration

8.1 The schematic and dimension of the standard C(T) specimen and the additional specimens are shown in Fig. A1.3.

8.2 The configurations and size range of all the geometries are given in Table A1.1.

8.2.1 Crack opening slot is the machined crack width. For C(T) specimens it can be as much as 0.1 a/W. For the rest of

the geometries, which have shorter crack starters it is recommended to have an opening of 0.05 *a/W*.

8.2.2 The self consistency of the starter notch is important for repeatability and test comparison. The user should use an internally reproducible starter notch process to give comparable results within a specific test program. This is especially important for the CCI calculations.

8.2.3 The width-to-thickness ratio *W/B* for the C(T) specimen is recommended to be 2, nominally. Other *W/B* ratios, up to 8, may be used for thickness effect characterization; it is however important to note that the stress state may vary with thickness (see 1.1.7 and 5.9).

8.2.4 The initial crack size, a_o (including a sharp starter notch or pre-crack), shall be at least 0.45 times the width, *W*, but no greater than 0.55*W*. This may be varied within the stated interval depending on the selected force level for testing and the desired test duration.

8.3 *Side-Grooving*—In most cases 20 % side-grooving is sufficient to meet crack front straightness requirements (see 5.9, 6.2.2, and 8.4). However more or less side-grooving in specimens may be required depending on the ductility and crack growth behavior of the material. The depth of required side-grooves for a particular material might only be found by trial and error but a total reduction of 20 % has been found to work well for many materials. However, for extremely creep-ductile materials, a total side-groove reduction of up to 40 % may be needed to produce straight crack fronts. Any included angle of side groove less than 90° is allowed. Root radius shall be ≤ 0.4 ± 0.2 mm in order to produce nearly-straight pre-crack fronts; it is desirable, but not a requirement, to have the pre-cracking done prior to side-groove machining operation.

8.4 *Specimen Size*—There are no specific size requirements imposed in this method but considerations due to constraint effects should be taken into account. Also specimen size must be chosen with consideration to the material availability, capacity of the loading system, being able to fit the specimen into the heating furnace with sufficient room for attaching the necessary extensometers, and providing sufficient ligament size for growing the crack in a stable fashion to permit collection of crack growth data (see also 1.1.7, 1.1.10, 5.9).

8.5 *Specimen Measurements*—The specimen dimensions are given in Fig. A1.3 and Table A1.1. They shall be machined within the machining tolerances given in Fig. A1.1 and the dimensions should be measured before and after the test.

8.6 *Notch Preparation*—The machined notch for the test specimens (see 8.2.1) may be made by electrical-discharge machining (EDM), milling, broaching, or saw cutting. It is recommended that the last 0.1 *a/W* of the crack be machined using electro discharge machining (EDM) of a width of 0.1 mm. This will allow easier pre-cracking or further crack tip sharpening by EDM to the final crack starter size prior testing. See Note in Fig. A1.3.

8.7 Associated pre-cracking requirements are discussed in 8.8.

8.8 *Pre-Cracking*—EDM or Fatigue pre-cracking are two methods used to introduce a sharp crack tip starter. It is recommended, using electro-discharge machine (EDM) method, that a narrow slit (of 0.1 mm width) should be introduced to produce a sharp and even crack starter. Fatigue pre-cracking could be performed as long as it can be ascertained that the final crack front will be straight and flat and does not deviate from the crack plane. EDM is preferable for some creep-brittle materials such as inter-metallics (**29**) and certain geometries due to difficulties in growing cracks with straight fronts. There may be indications that the mode of pre-cracking could affect the initial slow CCG period (see 1.1.5) and that the use of EDM may give longer times for the initial crack growth period compared with fatigue pre-crack. However this has not been fully established (**43**).

8.8.1 Care must be exercised during pre-cracking by either method to avoid excessive damage at the notch root. Hereafter, the two methods for pre-cracking are described.

8.8.2 *EDM Pre-Crack*—This is the preferred mode of inducing a sharp straight-fronted pre-crack. The width of the EDM pre-crack shall not exceed 0.1 mm. Precautions must be taken to avoid any localized over-heating which may alter the microstructure of the material near the crack tip. A minimum EDM length of 0.05 *a/W* from a blunt notch is recommended.

8.8.3 *Fatigue Pre-Cracking*—Specimens may also be pre-cracked at room temperature or at a temperature between ambient and test temperature under fatigue forces with a R-Ratio preferably of 0.1.

$$P_f = \frac{0.4B_N\,(W - a_o)^2\,\sigma_{ys}}{(2W - a_o)} \tag{6}$$

8.8.3.1 For the final 0.64 mm (0.025 in.) of fatigue pre-crack extension, the maximum force shall be no larger than P_f or a value such that the ratio of stress intensity factor range to Young's Modulus ($\Delta K/E$) is equal to or less than 0.0025 $mm^{1/2}$ (0.0005 $in.^{1/2}$), whichever is less. The accuracy of the fatigue force value shall be within ±5 %. The force range shall be no less than 90 % of the maximum force. The stress intensity factor range, ΔK, may be calculated using equations provided in A2.2.

8.8.4 The maximum force during the last 0.5 mm (0.02 in.) of pre-fatigue crack extension must not exceed the force used during creep crack growth testing.

8.8.5 To facilitate fatigue pre-cracking at low stress ratios, the machined notch root radius can be approximately 0.075 mm (0.003 in.). It may at times be expedient to have an EDM notch of 0.1 mm width to enhance the fatigue crack growth. A chevron form of machined notch as described in Test Method E399 or pre-compression of the straight through notch as described in Test Method E399 may be helpful when control of crack shape is a problem.

8.8.6 Pre-cracking is to be done with the material in the same heat-treated condition as that in which it will be tested for creep crack growth behavior. No intermediate heat treatments between pre-cracking and testing are allowed.

8.8.7 The size of the pre-crack extension from the machined notch shall be no less than 0.05 *a/W*.

8.9 *Specimen Preparation for Electric Potential Measurement:*

8.9.1 The stability of the PD system both due to the electronics and environmental changes is very important in CCG testing as the period of some tests are measured in months or possibly years. It is possible to determine the stability by placing a second PD probe remote from the crack to check the reference signal change which is independent of any crack growth. In this way if there is found to be a difference the main PD crack signal can be subtracted from the reference signal.

8.9.2 The specific recommendations for the C(T) specimen is presented in Annex A4 and detailed in reference **(53, 54)**. It should be noted that for all the geometries in Fig. A1.1 it is recommended to follow the procedures set out here.

NOTE 4—The C(T) PD analysis is a special case which has only been validated for a case specific situation **(53)** and it may not be applicable for every conditions. Therefore the user should proceed with Annex A4 with caution.

8.9.3 For gripping fixtures and wire selection and attachment also refer to the Annex in Test Method E647.

8.10 *Attachment of Thermocouples and Input Leads:*

8.10.1 The potential drop could be AC or DC powered. The input should be remote from the crack either welded or screw threaded. See Fig. A1.3 for C(T) specimen geometry.

8.10.2 A thermocouple must be attached to the specimen for measuring the specimen temperature. The thermocouple should be located in the un-cracked ligament region of the specimen 2 to 5 mm (0.08 to 0.2 in.) above or below the crack plane. Multiple thermocouples are recommended for specimens wider than 50 mm (2 in.). These thermocouples must be evenly spaced over the un-cracked ligament region above or below the crack plane as stated above.

8.10.3 In attaching thermocouples to a specimen, the junction must be kept in intimate contact with the specimen and shielded from radiation, if necessary. Shielding is not necessary if the difference in indicated temperature from an unshielded bead and a bead inserted in a hole in the specimen has been shown to be less than one half the permitted variations in 10.3.2. The bead should be as small as possible and there should be no shorting of the circuit (such as could occur from twisted wires behind the bead). Ceramic insulators should be used in the hot zone to prevent such shorting.

8.10.4 Specifications in Test Methods E139 identify the type of thermocouples that may be used in different temperature regimes. It is important to note that creep crack growth test durations are invariably long. Thus, a stable temperature measurement method should be used to reduce experimental error.

9. Calibration and Standardization

9.1 Performance of the electric potential system, the force measuring system, the temperature measurement systems and the displacement gage must be verified. Calibration of these devices should be as frequent as necessary to ensure that the errors for each test are less than the permissible indicated variations cited in this standard. The testing machine should be calibrated at least annually or, for tests that last for more than a year, after each test. Instruments in constant (or nearly constant) use should be calibrated more frequently; those used occasionally must be calibrated before each use.

9.1.1 Calibrate the force measuring system according to Practices E4 and E74.

9.1.2 Calibrate the displacement gage according to Method E83.

9.1.3 Verify electric potential system according to guidelines in Annex A4 and recommendation in Section 11.

9.1.4 Calibrate the thermocouples according to Test Method E220.

10. Test Procedure

10.1 *Plans for a Test Matrix*—A test matrix should be setup identifying, as far as possible, the goals for the tests such as the planned test times, available specimens, number of tests and the force levels that may be needed for the tests. Availability of spare specimens is essential as repeat tests may be required in some instances.

10.2 *Number of Tests*—Creep crack growth rate data exhibit scatter. The *da/dt* values at a given value of $C^*(t)$ and C_t can vary by as much as a factor of 2 **(45, 52)** for creep-ductile materials if all other variables such as geometry, specimen size, crack size, loading method and temperature are kept constant. For creep-brittle materials, the scatter in *da/dt* versus *K* relationship can be up to a factor of 4 **(35)**. This scatter may be increased further by variables such as micro-structural differences, force precision, environmental control, and data processing techniques. Therefore, it is good practice to conduct replicate tests; when this is impractical, multiple specimens (at least 4) should be planned such that regions of overlapping *da/dt* versus $C^*(t)$, C_t or *K* data are obtained. Confidence in the inferences drawn from the data will increase with the number of tests and the number of tests will depend on the end use of the data.

10.3 *Specimen Installation:*

10.3.1 Install the specimen on the machine by inserting both pins, then apply a small force (approximately 10 % of the intended test force) to remove slack from the loading train. Connect the current input and voltage leads to the current source and potentiometer, respectively. Attach the displacement gage to the specimen and the thermocouple to the appropriate potentiometer. Bring furnace into position and start heating the specimen.

10.3.2 Choose the appropriate force that will give the required specimen failure times. This can be calculated using previous tests of the same batch if available or estimated from available data in the literature on similar materials. If none is available the first test should be tested with incremental force increases to identify the failure force levels.

10.3.3 As an example the initial *K* (to compare to fracture toughness levels) and references stress (to compare to creep rupture times of uniaxial specimens) at force-up would give a good indication of the test lifetimes for most alloys **(12, 13)**.

10.3.4 Before the test force is applied and for the duration of the test, do not permit the difference between the indicated temperature and the nominal test temperature to exceed the following limits: *(a)* Up to and including 1000°C (1800°F) ±2°C (±3°F) above 1000°C (1800°F) ±3°C (±5°F). *(b)* The

term "indicated temperature" means the temperature indicated by the temperature measuring device using good quality pyro-metric practice.

NOTE 5—It is recognized that the true temperature may vary more than the indicated temperature. Permissible indicated temperature variations in 10.3.5 are not to be construed as minimizing the importance of good pyro-metric practice and precise temperature control. All laboratories should keep indicated and true temperature variations as small as practical. It is well recognized, in view of the extreme dependency of material properties to temperature, that close temperature control is necessary. The limits prescribed represent ranges that reflect common practice.

10.3.5 Temperature overshoots during heating should not exceed the limits above. It may be desirable to stabilize the furnace at a temperature from 5 to 30°C (10 to 50°F) below the nominal test temperature before making final adjustments. Report any temperature overshoot with regard to magnitude and duration.

10.3.6 The time for holding at temperature prior to start of test should be governed by the time necessary to ensure that the temperature can be maintained within the limits specified in 10.3.4. This time will not be less than one hour per 25 mm (1 in.) of specimen thickness. Report the time to attain test temperature and the time at temperature before loading.

10.3.7 Any positive temperature excursion beyond the limits specified in 10.3.4 is cause for rejection of the test. Negative temperature excursions wherein temperature falls below the specified limits should not be cause for rejection. Low temperatures do not induce the potentially adverse material changes associated with elevated temperatures. It is recommended that the crack growth data obtained during the low temperature excursion and during the period corresponding to 0.5 mm (0.02 in.) of crack extension following stabilization of the temperature be considered invalid and excluded.

10.3.8 The current for the electric potential system should be turned on at the same time as the furnace. This is necessary to ensure that resistance heating of the specimen caused by the applied current also stabilizes as the specimen is brought up to the test temperature.

10.4 *Loading Procedures:*

10.4.1 For constant force testing, a small fraction of the test force (not exceeding 10 %) may be applied before and during heating of the specimen. This procedure usually improves the axiality of loading by reducing the displacement caused by lateral forces.

10.4.2 Apply the test carefully so that shock forces or inertial overloads are avoided. The force should be applied in increments and the displacement and the PD should be monitored to ensure that the extensometer is properly seated and the information is available for post-test analysis. The time for application of the force should be as short as possible within these limitations.

10.5 *Measurements During the Test*—The electric potential voltage, force, force-line displacement, and test temperature should be recorded continuously during the test if autographic strip chart recorders are used. If digital data acquisition systems are used, the frequency of sampling should be no less than a full set of readings every fifteen minutes. More data points should be acquired during the periods of rapid change, namely the beginning and the final period of the tests. Regardless of the number of data points acquired the data will be reduced to a manageable amount in accordance with 12.1 and 12.1.9.

NOTE 6—If dead-weight creep machines are used for conducting the tests, it is not necessary to make force measurements.

NOTE 7—If dc current potential technique is used, then no current voltage (see Annex A1) should be measured. These measurements should be made at least once every 24 h.

10.6 *Post-Test Measurements:*

10.7 The test should be stopped when the crack length reaches 0.7 *a/W* or as soon as both the potential drop and the displacement measurement indicate that the tertiary stage of crack growth has begun and that final failure of the specimen is imminent. This region can be estimated from continuous monitoring of the data when the displacement and the PD are both increasing in relation to the previous steady state period. It is highly recommended to terminate a test prior to fracture because the final crack front is delineated more clearly and can be accurately measured for verifying the potential drop measurement. It will also allow for better metallographic analysis.

10.7.1 When the test is complete or stopped, remove the force and turn off the furnace. After the specimen has cooled down, remove the specimen from the machine without damaging the fracture surface.

10.7.2 If the specimen did not fracture at the end of the test, it should be broken open taking care to minimize additional permanent deformation. Ideally the specimen should be halved using EDM before breaking open one half of it. This will allow one half to be used to derive the exact value of the final crack size a_f which can be used in section for crack growth determination. And the other half could be used for metallographic purposes, before being broken, to observe the damage at the crack tip. The use of cyclic loading to break open the specimen is recommended. Also, ferritic steels may be cooled to a temperature below the ductile-brittle transition and fractured.

10.7.3 Along the front of the pre-crack and the front of the marked region of creep crack growth, measure the crack size at nine equally spaced points centered on the specimen mid-thickness line and extending to 0.005*W* from the roots of the side-grooves. Calculate the original crack size, a_o, and the final crack size, a_f, as follows: average the two near-surface measurements, combine the result with the remaining seven crack length measurements and determine the average. The measuring instrument shall have an accuracy of 0.025 mm (0.001 in.).

11. Calculation Procedure

11.1 *Determination of Crack Size*—Prior applying the procedure described in Annex A4 for determining the crack size during the test as a function of time it is recommended to perform the following actions:

11.1.1 Determine that the shape of the crack front at the start and end of the test.

NOTE 8—The variation of the crack front shape (see 10.7.3) does not vary from the surface to the center by more than ±20 %. If this occurs use the larger value of crack size for a conservative estimate. If this occurs the

results will be less reliable and will have increased scatter. Plan to make changes to the next test based on the findings (see 5.9).

11.1.2 Observe that the crack does not deviate from the crack plane parallel to the root of the side-groove by more than 20 %. If this occurs the results will be less reliable and will have increased scatter. Plan to make changes to the next test based on the findings (see 5.9).

11.2 Calculate the crack extension, a_t, by subtracting the observed initial crack size, a_o, from the value of the observed final crack size, a_f. The final crack size shall be determined from surface fractography measurements where possible (see 10.7.2).

11.2.1 Calculate crack growth with time as shown in A4.1. The crack size can be determined by linear interpolation of the electric potential readings using the initial crack size, a_o, and the final crack size, a_f.

11.2.2 If failure of the specimen occurs prior to the stoppage of the test then fractography measurements of the final crack size may not be possible. In this case follow the procedure described in A4.4 using the predictive formula for the C(T) specimen or follow A4.2 and A4.3 to estimate a_{pf} for the test.

11.2.3 If a_f is known then using the predictive method (valid only for the C(T)) to derive δa_{pf} in A4.4, is valid if:

$$0.85 \le \left(\frac{\delta a_{pf}}{(a_f - a_o)} \right) \le 1.15 \tag{7}$$

11.2.4 If a_f is unknown, a check using this equation is not possible. It is recommended that measurements from tests in question be compared with other valid data under similar conditions prior to inclusion in the data set.

NOTE 9—All variations from the recommended norms will at best produce increased scatter in the results and at worse be invalid. Therefore it is suggested where possible to repeat dubious tests.

11.2.5 All temperature excursions must be within the allowable levels in 10.3.5, otherwise the test is not valid.

11.3 *Determination of Time to Crack Extension $t_{0.2}$, Crack Growth Rate da/dt and Force-Line Displacement Rate dV/dt:*

11.3.1 From the recorded crack size and force-line deflection versus time results, choose the following data for further processing. The first data point consists of the pre-crack size with the corresponding time and accumulated deflection set at zero. Choose subsequent data points consisting of crack size and the corresponding force-line displacement and time, such that the minimum crack extension between successive data points is 0.25 mm (0.01 in.) and the minimum increment in deflection is 0.1 % of the full range of the extensometer. The maximum allowed δa between successive readings is $0.02W$. For recommendations on data reduction and data smoothing see 12.1.9. Following data smoothing, from the data identify the initial crack extension of δa = 0.2 mm and record the corresponding time to this crack length ($a_o + \delta a$). In general more than 20 smoothed data points per test does not contribute to accuracy but may produce fluctuations in the CCG and C^* data. However if the raw data does present a legitimate crack variation with time showing slow down and acceleration during the test the smoothed data should take it into account.

11.3.2 The creep crack growth rate and the force-line displacement rate can be determined from the crack size versus time (a versus t) and the force-line displacement versus time (V versus t) data. Recommended approaches that utilize the secant or incremental polynomial methods are given in Appendix X1.

NOTE 10—Both recommended methods for processing a versus t and V versus t data are known to give similar da/dt or $\dot{a}$ and dV/dt or $\dot{V}$ response. However, the secant method often results in increased scatter in da/dt and dV/dt relative to the incremental polynomial method, since the latter numerically smoothes the data. This apparent inconsistency introduced by the two methods needs to be considered since it will contribute in the overall scatter of the data.

11.4 *Calculation of the Appropriate Displacement Rate:*

11.4.1 The total displacement rate dV/dt is recommended to be used in the analysis of C^* (see 11.8). However this is only valid if the criteria in 11.8.1 and 11.8.3 are met. This means that if then creep dominates and the errors involved in using the total dV/dt are well within experimental data scatter. The displacement rate can be either from Force-line (*FLD*) or Crack Mouth Opening (*CMOD*) positions.

NOTE 11—Guidelines in estimating the plasticity component are provided in Appendix X2 for the C(T) specifically. These can be used to identify whether plasticity will invalidate the test or assist in faster redistribution of the crack tip stresses.

11.5 *Calculation of the K and C* Parameters*—Annex A2 gives the details for the recommended solutions for determining K and C^*. It is evident from the literature that there are varying techniques available for the evaluation of K and C^*. The differences that may be observed in terms of K are usually not greater than ±10 %. However due to the high stress sensitivity in the creep process these differences can be considerably larger when comparing different C^* evaluation methods.

11.6 *Valid and Recommended Solutions*—The optimum solutions for C^* for the different geometries have been presented in Annex A2 with the knowledge that other similar solutions may be available. However it is essential to have uniformity in the method of analysis as well as the use of consistent formulae. The improved use of inter-laboratory data and life assessment analysis methods will depend on this recommendation since the analyses can be carried out with more confidence and repeatability.

11.7 *Parameter Validity Criteria*—The choice of the most appropriate correlating parameter for initial crack growth (CCI) and steady state growth rate (CCG) depends mainly on whether the material exhibits creep-ductile or creep-brittle behavior **(12, 13, 29, 42)**. Steady-state creep crack growth rates in creep-ductile materials are correlated by C^*. C_t or $C^*(t)$ for the present geometries shown in Fig. A1.3 are comparable **(12, 13)**.

11.8 *C* Estimation*—This standard adopts the estimation of C^* as shown in Annex A2 when steady state regime prevails for which C^* during the steady state period is self-similar to either the $C^*(t)$ or C_t. For the steady-state creep crack growth rates in creep-brittle materials K is recommended (see 11.8.1 on validity criteria) as an engineering compromise and for the simplicity of the method and the availability of solutions. A more rigorous solution would be to use C_t **(13, 33)** as it is the parameter that can represent small-scale creep. This method is not validated in this standard.

11.8.1 To identify the valid regions for C^* and K the ratio of $\dot{V}_c / \dot{V}$ should be calculated for each point. An estimate can be made also by partitioning the components using Eq 8. See 11.8.3 for recommendations. If $\dot{V}_c / \dot{V} \geq 0.5$, the data are classified as being creep-ductile and the candidate crack growth rate relating parameters C^* is recommended using the total displacement rate. If $\dot{V}_c / \dot{V} \leq 0.25$ the data are classified as being creep-brittle then the candidate parameter K is used and the user must use A2.3 for further evaluation of the data.

11.8.2 In order to estimate this ratio it should be assumed *(a)* that the plastic component in Eq 3 is small (that is, analysis should be for long term tests and low test forces) and *(b)* that plasticity will instantaneously relieve the stresses at the crack tip and assist in reducing the redistribution time for C^* as is probable at the crack tip.

11.8.3 On the above basis the total force-line displacement rate, $\dot{\Delta}$, can be partitioned into an instantaneous (elastic) part, $\dot{\Delta}_e$, and a time dependent part that is directly associated with the accumulation of creep strains, $\dot{\Delta}_e$ can be obtained by:

$$\dot{\Delta}_e = \frac{\dot{a}B}{P}\left[\frac{2K^2}{E'}\right] \tag{8}$$

where:

$\dot{a}$ = crack growth rate,
P = applied force,
B = specimen thickness,
K = stress intensity factor, and
E' = elastic constraint modulus ($E/(1\text{-}\nu^2)$ for plane strain and E for plane stress.

11.8.3.1 For side grooved specimens B in Eq 8 should be replaced by B_N. Thus by deriving $\dot{V}_c / \dot{V}$ from Eq 8 and Eq 3 (assuming negligible plasticity) it is assumed that steady state, extensive creep conditions prevail, and that the data can be classified as being creep ductile when $\dot{V}_c / \dot{V} > 0.5$.

11.8.4 For the condition where $0.25 \leq \dot{V}_c / \dot{V} \leq 0.5$, where neither C^* nor K field are dominant it is advised to correlate *da/dt* with C^* and also with K in order to identify bounds and quality of correlation and report findings. A more detailed numerical analysis, which is not within the scope of the present standard, may assist in the analysis.

NOTE 12—The results may not be fully validated and/or correlated to the steady state C^* calculated using the technique proposed in Annex A2.

11.8.5 The second validity criterion is to verify data for which the time exceeds a transition time, t_T. Only data beyond this time period can be correlated versus the steady state C^*. The transition time t_T is estimated as shown in Eq 6 and discussed in 4.2.11, and below:

$$t_T = \frac{K^2(1-\nu^2)}{E(n+1)C^*(t_T)} \tag{9}$$

11.8.5.1 The calculation of t_T depends on the value of $C^*(t_T)$. Thus, the following procedure must be used for its estimation. For time, t, corresponding to each data point, calculate $\dot{t}_T$ using the above equation but substituting $C^*(t)$ for $C^*(t_T)$. t_T is then the largest value of $\dot{t}_T$ in the entire data set.

11.8.6 The data for which time is less than t_T, data can be correlated using K or C_t (using an elastic-creep analysis).

11.8.7 For crack growth rate data in creep-brittle materials to correlate with K, the following requirements must be met: *(a)* Data for an initial crack extension of < 0.2 mm must be disregarded (**29**). (This data can be used to estimate CCI.) *(b)* $\dot{V}_c / \dot{V} \leq 0.25$. If the data do not adhere to the above requirements then that data are not uniquely dependent on the magnitude of K and are not considered valid by this method. The scope of this standard does not cover creep brittle behavior where there is no steady state crack growth. However, under these circumstances the value of stress intensity factor K and time to 0.2 mm initial crack extension and final failure time should be recorded to compute initial crack growth (CCI). There are a number of methods under development (**39, 54-56**) for dealing with this condition.

11.8.8 Derivation of $t_{0.2}$ versus C^* relationship should use the value of calculated C^* at $a_o + \delta a$ (where $\delta a = 0.2$ mm). If the value of C^* has not reached steady state then this should be reported. It is likely that the scatter for $t_{0.2}$ *v* C^* data will be high. This is due to the parameter variability in the transient region, the error in estimating 0.2 mm of crack extension and the fact that C^* might not have reached steady state.

11.8.9 Where $\dot{V}_c / \dot{V} \leq 0.25$, then $t_{0.2}$ *v* K relationship should be used in the same manner as above.

11.8.10 Time to growth the crack $t_{0.2}$ from force-up may include only a portion of the transient region in creep-brittle materials and therefore the results will indicate more scatter and the results should be correlated with both C^* and K as a comparison. However for creep ductile materials where $\dot{V}_c / \dot{V} >> 0.5$ transition times are usually found to be $t_T << t_{0.2}$ (**29, 42, 43**).

11.9 *Further Validity Requirements:*

11.9.1 The time required to achieve the first 0.2 mm (0.008 in.) of crack extension during a constant force test is referred to as t_o. It may constitute all or part of the transient region. The crack growth behavior during the transient region is affected by creep damage development and in some creep-brittle materials can represent a substantial portion (up to as high as 80 %) of the test time (**35**). It is recommended that a record of the time, $t_{0.2}$, taken to reach a crack extension of 0.2 mm be made, and included as a part of the report with the appropriate value of C^* or K at the end of the crack extension of 0.2 mm. Any data gathered prior to 0.2 mm of crack extension must be excluded from data used to calculate *da/dt*.

11.9.2 If, during the test, the crack deviates outside an envelope that encompasses the material between the planes that are oriented at ±5° from the idealized plane of crack growth and that intersect the axis of loading, the data are invalid by this test method or the particular geometry or side-grooving chosen. It is therefore recommended that the test geometry should be changed and/or an increase in side-grooving considered.

11.9.3 Data acquired after the accumulated force-line deflection, exceeds 0.05W, which could be due to either creep or plasticity, are considered invalid by this test method. The problem could be avoided by an increase in side-grooving, initial crack size and a geometry change, effectively increasing crack-tip constraint.

12. Report of Findings

12.1 Report the following information:

12.1.1 Specimen type and dimensions including thickness, B, net thickness, B_N (if side-grooved) and width, W.

12.1.2 Description of the test machine and equipment used to measure crack size and the precision with which crack size measurements were made.

12.1.3 Test material characterization in terms of the heat treatment, chemical composition, tensile properties at room temperature and test temperature, the pre-exponent A and the creep exponent n (for the Norton relationship giving the creep strain rate $\dot{\varepsilon} = A\sigma^n$) used in calculations, including how it was derived. Also identify product size and form (for example, sheet, plate, and forging).

12.1.4 *Crack Plane Orientation*—In addition, if the specimen is removed from a large product form, give its location with respect to the base material.

12.1.5 The terminal value of K, P_{max}, P_{min}, the pre-cracking temperature, and the frequency of loading and the number of cycles used for fatigue pre-cracking. If pre-crack forces were stepped-down, state the procedure employed for the loading method and give the amount of crack extension at the final force level. If an EDM notch is used in-lieu of a fatigue pre-crack, report the root radius and the length of the notch.

12.1.6 State test force and experimental variables such as test temperature and environment. For environments other than laboratory air, report the chemical composition of the gas.

12.1.7 Record force-up information at the start of the test and force-down at the end of a stopped test.

12.1.8 Report the data analysis methods, including the technique used to convert crack size and deflection data into rates and the specific procedure used to correct for discrepancies between measured crack extension on the fracture surface with that predicted from the electric potential method.

12.1.9 Since sometimes continuous data are acquired in a creep test the raw data should be plotted and reduced in an orderly fashion to between recommended 25-35 points. More data should be present in the early and final stages of the test as the rapid changes occur at those regions.

12.1.10 Any smoothing of data should be made to reduce scatter and measuring fluctuations and not possible changes in the cracking or deformation behavior of the specimen. The smoothed data of crack size, displacement against time should then be used to derive the required slopes. See Appendix X1 for methods to derive the slopes for *da/dt* and *dV/dt*.

12.1.11 The displacement rates that are derived are used in Annex A2 to derive C^*.

12.1.12 Plot *da/dt*, versus C^* or K. It is recommended that C^* be the abscissa and *da/dt*, be the ordinate. Log-Log co-ordinate axes are normally used. Report all data that violate the validity criteria in 11.1 – 11.9.3 and identify.

12.1.13 Report crack growth time at force-up, $t_{0.2}$, for the crack to extend by $\delta a = 0.2$ mm at the beginning of a test and recorded the appropriate K and C^* at crack size $a_o + \delta a$. Also report the mode of pre-cracking either by EDM or Pre-Fatigue as it may affect the result.

12.1.14 Description of any occurrences that appear to be related to anomalous data (for example, transient behavior following test interruptions or changes in force levels).

12.1.15 It is desirable, to tabulate test results and the corresponding analyzed data. When using this test method for presentation of results, the following information should be tabulated for each test: a, t, *da/dt*, *dV/dt*, C^*, K, t_T, $t_{0.2}$ at δa = 0.2 mm of crack from the start of loading.

12.1.16 Calculate the mean slope and standard deviation of the dataset from the log/log plots of the *da/dt v* K or C^* and $t_{0.2}vK$ or C^* data.

13. Precision and Bias

13.1 *Precision*—The precision of *da/dt*, versus C^*or K is a function of inherent material variability as well as errors in measuring crack size, temperature, creep displacement rates and applied force levels.

13.1.1 In general the crack size errors cause significantly less of a contribution to the variability in *da/dt* except in the early stages of cracking where crack size extensions are <0.2 mm which is below the recommended crack size measurement sensitivities recommended. In fact the test to test variability on the same material batch could give a wider scatter (as much as a factor of 4) in the crack growth rate data than the actual errors involved in the measurement of force, displacement and crack size.

13.1.2 The variability due to the derivation of K could be as much as ±10 %. But in evaluating C^* this difference could be as much as a factor of ±25 % at best for each geometry identified in Fig. A1.3. This bigger difference is due to the variability in deriving an appropriate η factor and in the applied force on the specimen (especially from the applied from a servo-hydraulic test). There will also exist an additional small divergence in C^* due to unresolved differences that may exist in deriving $C^*(t)$, C_t. Such factors cannot be fully ascertained at the present time and order to compensate for these differences the adoption of specific formulae of the C^* parameter for the different geometries in this standard will allow inter-laboratory comparisons without the need to question the detail in the possible unresolved differences that presently exist in the C^* estimation procedure.

13.1.3 Although it is often impossible to separate the contributions from each of the above mentioned sources of variability, an overall measure of variability in *da/dt*, versus C^*, $C^*(t)$, C_t or K is available from the results of an inter-laboratory test programs **(29, 30)**. Some of these data, for example, obtained on highly homogeneous 1 Cr-1 Mo-0.25 V steel at 594°C (1100°F), showed the reproducibility in da/dt versus C^*, $C^*(t)$ or C_t under controlled conditions to be ±25 %. However these differences can be as much as a factor of 4 in inhomogeneous material specifications and in materials which are creep brittle.

13.1.4 It is important to recognize that for the purposes of design or remaining life assessment, inherent material variability often becomes the primary source of scatter in *da/dt*. The variability associated with a given lot of material is caused by inhomogeneity in chemical composition, microstructure and the local creep properties, or all of them. These same factors

coupled with varying processing conditions give rise to further batch to batch differences in cracking rates (**10**, **31**). An assessment of inherent material variability, either within or between heats or lots, can be determined only by conducting a statistically planned test program on the material of interest. Thus, the results cited above from the inter-laboratory test programs utilizing materials selected to minimize material variability allow assessment of measurement precision, but are generally not applicable to questions regarding inherent variability in other materials.

13.2 *Bias*—There is no accepted "standard" value for CCI (t_i) or CCG rate (da/dt) versus C^*, $C^*(t)$, C_t, K for any material. In the absence of such true value, no meaningful statement can be made concerning bias of data.

ANNEXES

(Mandatory Information)

A1. FIGURES

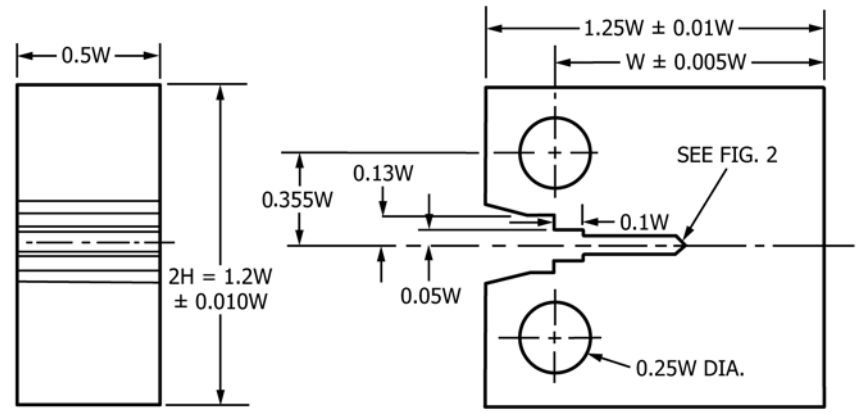

COMPACT TEST SPECIMEN FOR PIN OF 0.24W (+0.000W/ –0.005W) DIAMETER

FIG. A1.1 Drawing of a Standard C(T) Specimen with the Machining Tolerances

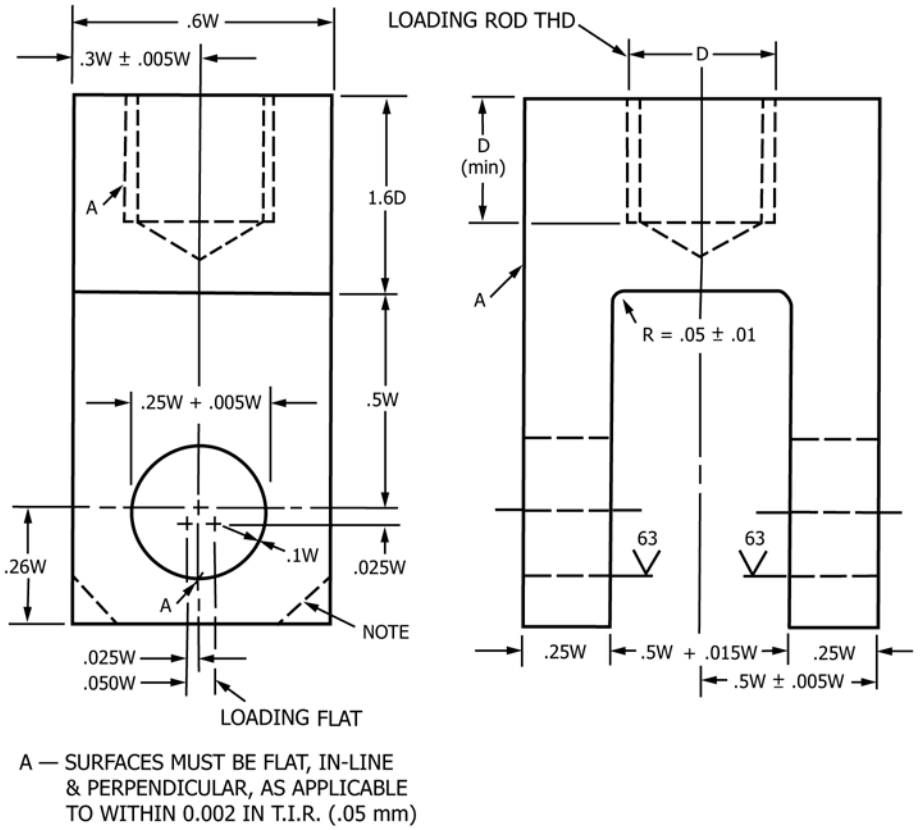

NOTE 1—Corners of the clevis may be removed as necessary to accommodate the clip gage.

FIG. A1.2 Example of Clevis Assembly for Tension Specimens with Machining Tolerances

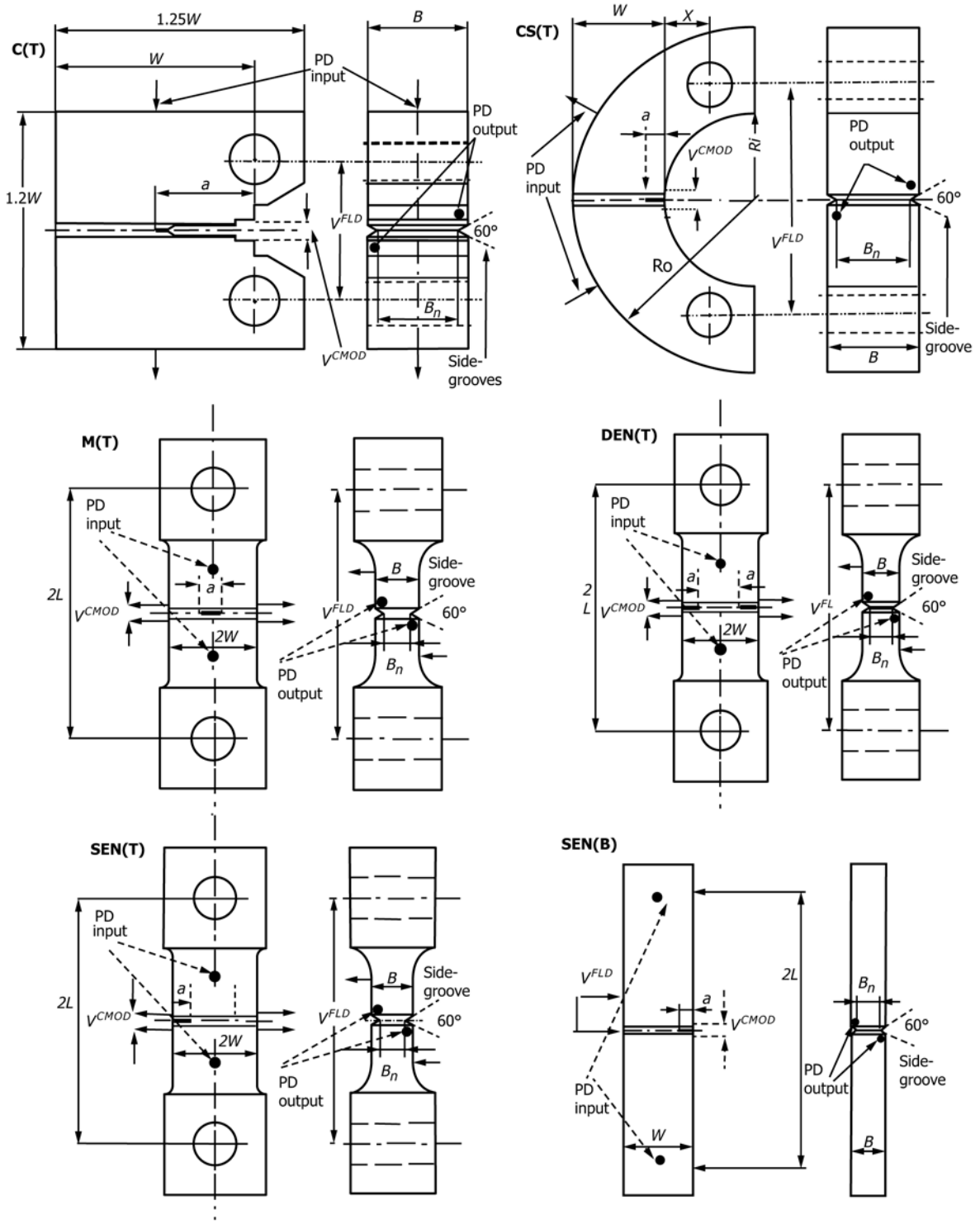

NOTE 1—This schematic does not represent the true crack opening dimensions. Crack machining should follow the direction laid down in Fig. A1.1 followed by a sharp EDM cut with a thickness of 0.1 mm. Since the initial cuts are machined with a wider thickness then the final 0.1 *a/W* to the crack tip must be no wider than 0.1 mm. This is important since CCI and CCG are profoundly affected by crack notch width.

FIG. A1.3 Schematic Drawings for the Six Fracture Mechanics Geometries Showing the Force Directions, and Force-Line Displacement V^{FLD} and Crack Mouth Opening Displacement V^{CMOD} Positions, the Weld Height Profile (if a weld specimen is used), the Potential Drop (PD) Input and Output Positions and Side-Grooves

TABLE A1.1 Specimen Abbreviations and Dimensional Range Shown in Fig. A1.3

Name	Specimen Definition	*W* (mm)	*B* (mm)	*H*, *L*, R_o (mm)
C(T)	Compact Tension	50	$W/2 \rightarrow W/4$	$H = 0.6W$
CS(T)	C-Shaped Tension	25	$W \rightarrow W/2$	$R_o = 2W$
SEN(T)	Single Edge Notched Tension	25	$W/2 \rightarrow W/4$	$L = 2W$
SEN(B)	Single Edged Notched Bending	25	$W/2 \rightarrow W/4$	$L = 2W$
DEN(T)	Double Edge Notched Tension	12.5	$W \rightarrow W/2$	$L = 4W$
M(T)	Middle Tension	12.5	$W \rightarrow W/2$	$L = 4W$

In this table, *H* is half height of C(T), R_o is the outer radius, and $X = W/2$ for CS(T) and *L* is the half length of SEN(T), SEN(B), DEN(T) and M(T) specimens. A schematic illustration for each specimen geometry is shown in Fig. A1.3. In this figure in parallel with this table, the range of specimen dimensions are defined together with the loading configuration. The force line displacement, V^{FLD}, and crack mouth opening displacement, V^{CMOD} positions as well as the potential drop (PD) input and output positions and side-grooves of the geometries are also shown in Fig. A1.3.

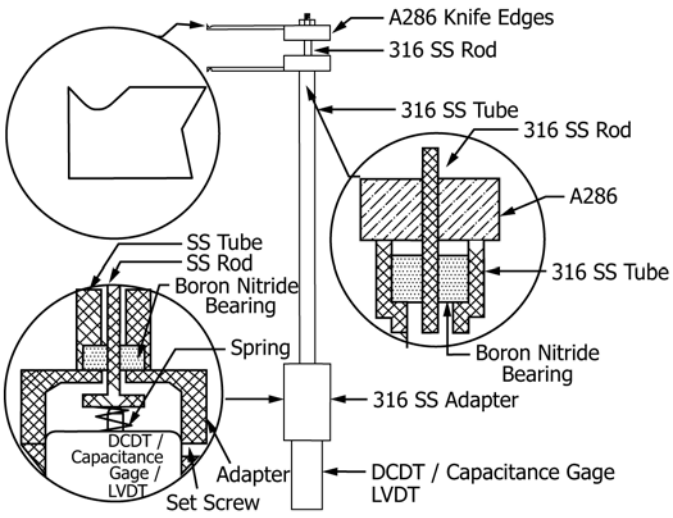

NOTE 1—The rod and tube must be made from the same material.

FIG. A1.4 Schematic of a Clip Gage Assembly for Measuring Force-Line (FLD) or Crack Mouth Opening (CMOD) Deflection in Different Geometries Using 316SS Steel as an Example

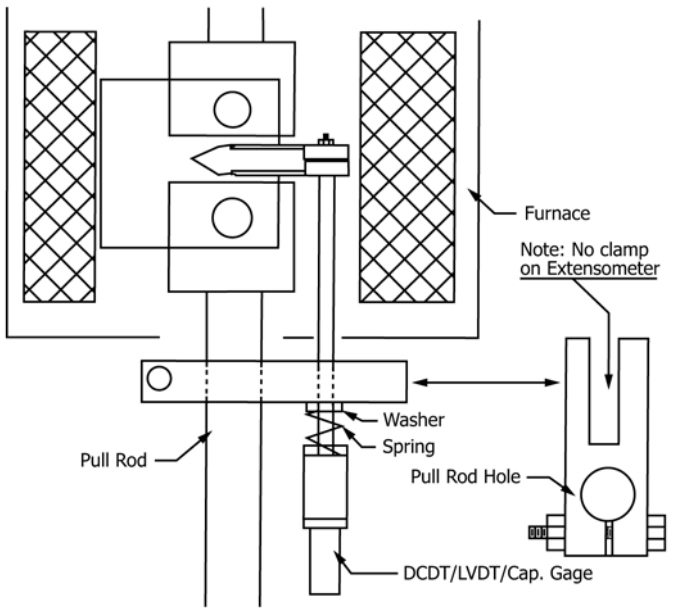

NOTE 1—The materials used in the shackles and clevis must be adequate for the test temperature.

FIG. A1.5 Schematic of an Overall Test Set-Up Showing the Clip Gage as Attached to the Specimen

A2. FRACTURE MECHANICS PARAMETER DETERMINATION

A2.1 *Specimen Fracture Mechanics Parameter Solutions*—In this section a detailed list of fracture mechanics parameters (K, C^*, η) used in the analysis of the data are presented for the specific geometries shown in Fig. A1.3 **(53-63)**. These are verified solutions which can be used in the analysis of creep crack growth data.

A2.2 Fracture mechanics parameter C^* is by far the most accepted method that is employed for the analysis of creep crack growth data. K is used in the rare cases where creep deformation and activation energy is low, usually occurring at lower creep temperature range. Both these parameters are validated and recommended in this standard.

NOTE A2.1—It should be noted that other parameters such as the material creep toughness parameter K^c_{mat} **(55, 56)** for crack initiation and the activation energy based Q^* **(57, 64)** for crack growth, CTOD **(45)** have been proposed and in some cases used. However these are yet to be fully established and validated and as such are not presented in this document.

A2.3 *Stress Intensity Factor K Solutions*:

A2.3.1 The linear elastic K is appropriate for creep brittle analysis is defined here for the geometries shown in Fig. A1.3. Since there are numerous references which tabulate or quote K values for different geometries **(55, 56)** and it is important to have an accurate and validated measure of K for each geometry.

A2.3.2 The general equation for stress intensity factor is given by:

$$K = Y(a/W)\sigma\sqrt{a} \tag{A2.1}$$

where:

σ = applied nominal stress,
$Y(a/W)$ = function of geometry,
a = crack size, and
W = geometry width, as defined in Table A1.1.

A2.3.2.1 When a specimen is side-grooved, the applied force will be acting over a shorter crack front and the stress intensity factor of a side-grooved specimen K_n, is given by:

$$K_n = K\sqrt{\frac{B}{B_n}} \tag{A2.2}$$

where:

B_n = net specimen thickness.

A2.3.2.2 *Solutions for the Y(a/W) Functions*—Eq A2.3-A2.17 contain the solutions for the geometries in Fig. A1.3. These equations also include equations for the membrane bending stresses for specimens loaded under a tensile force F and for specimens subjected to a constant bending moment M the nominal bending stress at the surface.

A2.3.3 *Y factor for C(T):*

$$Y = \sqrt{\frac{W}{a}}\left[\frac{2+a/W}{(1-a/W)^{3/2}}\right] f(a/W) \tag{A2.3}$$

$$f(a/W) = 0.886 + 4.64(a/W) - 13.32(a/W)^2 + 14.72(a/W)^3 - 5.6(a/W)^4 \tag{A2.4}$$

$$\sigma = \frac{F}{BW} \tag{A2.5}$$

where:

F = the applied force.

A2.3.4 *Y factor for CS(T):*

$$Y = \sqrt{\frac{W}{a}}\left[\frac{3X}{W} + 1.9 + 1.1\left(\frac{a}{W}\right)\right] \left[1 + 0.25\left(1 - \frac{a}{W}\right)^2\left(1 - \frac{R_i}{R_o}\right)\right] f(a/W) \tag{A2.6}$$

$$f(a/W) = \frac{\sqrt{a/W}}{(1-a/W)^{3/2}}\left(3.74 - 6.3(a/W) + 6.32(a/W)^2 - 2.43(a/W)^3\right) \tag{A2.7}$$

$$\sigma = \frac{F}{BW} \tag{A2.8}$$

where:

R_i and R_o = inner and outer radii, respectively, and
X = loading hole offset.

A2.3.5 *Y factor for SEN(T):*

$$Y = \sqrt{\frac{2W}{a}\tan\left(\frac{\pi a}{2W}\right)} \left[0.752 + 2.02\left(\frac{a}{W}\right) + 0.37\left(1 - \sin\left(\frac{\pi a}{2W}\right)^3\right)\right] / \cos\left(\frac{\pi a}{2W}\right) \tag{A2.9}$$

$$\sigma = \frac{F}{BW} \tag{A2.10}$$

A2.3.6 *Y factor for SEN(B) (3-Point Bend Specimen):* For Span = $4W$, that is $L/W = 2$.

$$Y = \frac{1}{(1+2a/W)(1-a/W)^{3/2}} \left[1.99 - \frac{a}{W}\left(1 - \frac{a}{W}\right)\left(2.15 - 3.93\frac{a}{W} + 2.7\left(\frac{a}{W}\right)^2\right)\right] \tag{A2.11}$$

$$\sigma = \frac{3FL}{BW^2} \tag{A2.12}$$

A2.3.7 *Y factor for DENT(T):*

$$Y = \sqrt{\frac{2W}{a}\tan\left(\frac{\pi a}{2W}\right)}\left[1 + 0.122\cos^4\left(\frac{\pi a}{2W}\right)\right] \tag{A2.13}$$

$$\sigma = \frac{F}{2BW} \tag{A2.14}$$

For DEN(T) specimen the width W is replaced by $2W$.

A2.3.8 *Y factor for M(T):*

$$Y = \sqrt{\pi\sec\left(\frac{\pi a}{2W}\right)}\left[1 - 0.25\left(\frac{a}{W}\right)^2 + 0.06\left(\frac{a}{W}\right)^4\right] \tag{A2.15}$$

$$\sigma = \frac{F}{2BW} \tag{A2.16}$$

A2.4 *C* Solutions*—The parameter *C** can be calculated in a number of ways (**12, 13**). This procedure recommends that estimates of *C** should be obtained by experimental analysis methods set out below. Therefore the procedure to derive *C** described in this section is recommended and applicable to laboratory specimens shown in Fig. A1.3 and identified in Table A1.1.

A2.5 The data derived using this method can act as 'Benchmark' material properties data which can then be used for design and life assessment purposes. This allows for a reduction in errors and scatter due to the use of different estimation methods which themselves be valid but give a different value to the present solutions. It is recommended therefore that *C** is calculated from the general relationship:

$$C^* = \frac{F\,\dot{\Delta}}{B_N(W-a)}\,F' \tag{A2.17}$$

where:

$\dot{\Delta}$ = total force-line displacement rate,
F' = non-dimensional factor which is a function the uniaxial creep properties index n and a geometry dependent factor (which can be obtained from limit analysis techniques),
B_N = net thickness of the specimen with side-grooves, and
W = width.

A2.5.1 In general, Eq A2.17 is used to estimate the values of *C** assuming $\dot{V}_c \cong \dot{V}$. Factor F' can be given by:

$$F' = -H\,\frac{1}{F_L}\,\frac{dF_L}{d(a/W)} \tag{A2.18}$$

where:

H = function of the creep index n and geometry, and
F_L = limit force.

A2.5.2 Hence, *C** can be re-expressed as:

$$C^* = \frac{F\,\dot{\Delta}}{B_N(W-a)}\,H\eta \tag{A2.19}$$

where:

$$\eta = -\frac{1}{F_L}\,\frac{dP_L}{d(a/W)} \tag{A2.20}$$

A2.5.3 *C** can be calculated, by replacing in Eq A2.19 the appropriate displacement rate. Therefore $\dot{\Delta}^{FLD}$ and $\dot{\Delta}^{CMOD}$ which are respectively the force-line and crack mouth opening displacement rates can be used to estimate *C** giving:

$$C^* = \frac{P\,\dot{\Delta}^{FLD}}{B_N(W-a)}\,H^{FLD}\eta^{FLD} \tag{A2.21}$$

$$C^* = \frac{P\,\dot{\Delta}^{CMOD}}{B_N(W-a)}\,H^{CMOD}\eta^{CMOD} \tag{A2.22}$$

NOTE A2.2—See Fig. A1.3 for the positions where the force-line (*FLD*) or Crack Mouth Opening (*CMOD*) are measured.

A2.6 The definitions for H^{FLD} and H^{CMOD} are given in Table A2.1 and the recommended η^{FLD} and η^{CMOD} functions using the above equations have been derived numerically (**46, 60-63, 65-67**) for the geometries shown in Fig. A1.3. The recommended η factors for the valid crack length range are also given as actual values and equations in Tables A3.1 and A3.2 respectively for all the geometries and a range of weld mismatch factors of $0.5 \le M \le 2$. With M = 1 being the homogenous properties. See further discussions on the weldments testing section below.

A2.7 For the cracked geometries considered, the value of η^{FLD} and η^{CMOD} is found to be sensitive to the creep exponent, n, and relative specimen height, L/W and stress state. However an extensive numerical analysis carried out and compared with other results in the literature (**64**) suggest that there is no clear trend or relationship can be identified with these variables and the η^{FLD} and η^{CMOD}. Therefore mean values η^{FLD} and η^{CMOD} with respect to a/W for different weld mismatch ratios are quoted and given as equations in Tables A3.1 and A3.2 identifying mean and upper/lower bounds for η. The user should normally apply the mean values in the analysis. Should the user need to compare results with the upper/lower bound solutions depending on the level of conservatism that is needed, it is recommended that both analyses are carried out. It is however unlikely that η^{FLD} and η^{CMOD} values will have a major effect on the *C** solutions. It is recommended that the evaluation of crack growth should correspond to this range as the errors involved outside the region may render the evaluation of *C** as prone to further errors.

TABLE A2.1 Definition of *H* for Each Configuration (11, 23)

Specimen Type	H^{CMOD}	H^{FLD}
C(T)	$N/(N+1)$	$N/(N+1)$
CS(T)	$N/(N+1)$	$N/(N+1)$
SEN(T)	$N/(N+1)$	$N/(N+1)$
SEN(B)	$(2L/W)N/(N+1)$	$N/(N+1)$
DEN(T)	$1/2(N-1)/(N+1)$	$1/2(N-1)/(N+1)$
M(T)	$1/2(N-1)/(N+1)$	$1/2(N-1)/(N+1)$

A3. FURTHER RECOMMENDATIONS FOR TESTING SPECIMENS CONTAINING WELDS

A3.1 Further Recommendations for Testing Specimens Containing Welds

A3.1.1 There are cases when crack growth rates for weldment properties will be needed. This annex gives recommendations for dealing with such cases. Fig. A1.3 shows for the relationship of the weld height region with respect to the crack center for the six recommended specimens. The half weld height h can be as wide as the half of the specimen or a very thin line depending on the type of weld. The important point to note is that the region to be tested must be configured in the crack growth line center path of the geometry. Therefore if the HAZ region is to be tested, the specimen must be cut accordingly as shown schematically in Fig. A3.1. The weld region can be simply categorized as the weld material or heat affected zone (HAZ) interfacing the parent base material. In the HAZ region the grain sizes vary for most welds. The size of the weld and the HAZ region would vary according to the method of welding and the size of the weld. It should be noted that in testing these specimens, an improved material crack growth characterization of the specific region of the weld or HAZ region can be derived.

A3.1.2 Welding is usually expected to contain residual stresses which should ideally be taken into account in the derivation of the fracture mechanics parameters. However it has been shown that post weld heat treatment (PWHT) of specimens would drastically reduce the residual stresses. In addition it has also been shown (**65**) that even with no PWHT the steps needed to first cut the specimen from the block and secondly to machine and cut the pre-crack in the specimen will substantially reduce residual stresses. This will mean that the residual stresses in the laboratory specimens need not be considered, for tests < 5000 hours duration, as the machining and the creep relaxation at temperature will rapidly reduce the secondary stresses and the primary force can be assumed to be the main force to drive the crack under creep conditions.

A3.1.3 Analyzing CCI in weldments it is assumed that a growth to a crack depth of 0.2 mm, similar to that for homogenous materials, would give the time for crack initiation. If the crack is shown to deviate from the crack path the results may not be used for CCI or CCG properties of the region of interest in the weld. Then the test becomes invalid and if the crack deviates from the pre-designated path then the test becomes invalid and should be repeated or redesigned. It is also clear that given the inhomogeneity of the material at the crack tip there will be substantially more scatter of the data when compared to as received base steels. It is therefore suggested that repeat tests should be performed.

A3.1.4 It should be noted that the correlating parameter K and C^* is also appropriate for inhomogeneous specimens providing the C^* criteria described in the analysis Section 11 are met. Tables A3.1 and A3.2 give, where available calculated values of η^{CMOD} and η^{FLD} for specific values of a/W in the six welded geometries with respect to crack length as a list and equations, respectively. These calculations, within the range of

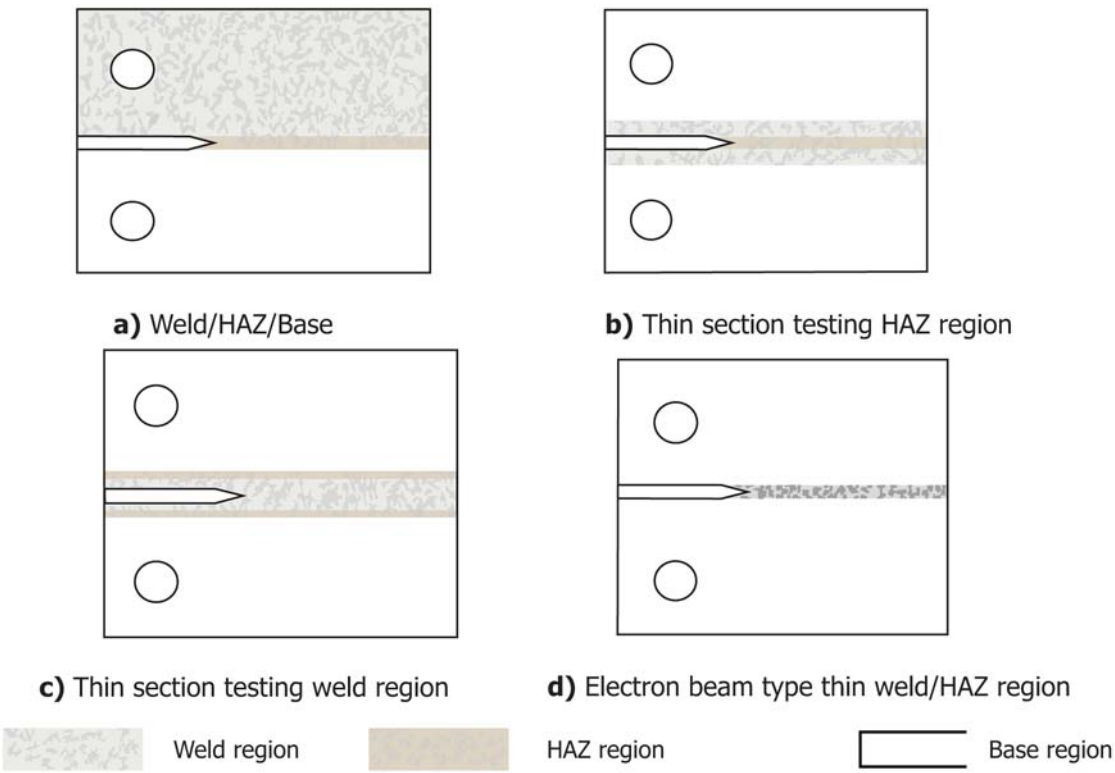

FIG. A3.1 Schematic Configurations of Welded Specimens that Could Be Used to Measure Cracking

TABLE A3.1 Calculated Values of η^{CMOD} and η^{FLD} for Specific Values of *a/W* for Standard Fracture Mechanics (66, 67) Specimens C(T), CS(T), SEN(T), SEN(B), DEN(T), M(T) in Fig. A1.3 Giving the Mean and Upper/Lower Bound Deviations

η^{FLD} *a/W*	C(T) base (±0.10)		UM - (*M*=0.5) (±0.20)		OM - (*M*=1.5) (±0.18)		OM - (*M*=2) (±0.14)	
0.35	1.89		2.24		1.73		1.63	
0.40	2.07		2.35		1.92		1.81	
0.45	2.20		2.61		2.10		2.00	
0.50	2.20		2.61		2.10		2.00	
0.60	2.20		2.6		2.10		2.00	
0.70	2.20		2.6		2.10		2.00	
a/W	CS(T) base		UM - (*M*=0.5)		OM - (*M*=1.5)		OM - (*M*=2)	
	η^{CMOD} (±0.16)	η^{FLD} (±0.23)	η^{CMOD} (±0. 3)	η^{FLD} (+0.24)	η^{CMOD} (±0.17)	η^{FLD} (±0.22)	η^{CMOD} (±0.25)	η^{FLD} (±0.15)
0.20	4.08	2.05	4.52	2.31	3.84	1.89	3.61	1.60
0.30	4.08	2.16	4.52	2.38	3.84	2.00	3.61	1.79
0.40	3.92	2.27	4.27	2.45	3.68	2.11	3.45	1.98
0.50	3.76	2.23	4.03	2.38	3.52	2.07	3.29	1.94
0.60	3.61	2.19	3.79	2.30	3.37	2.03	3.13	1.90
0.70	3.45	2.15	3.55	2.23	3.21	1.99	2.98	1.86
a/W	SEN(T) base		UM - (*M*=0.5)		OM - (*M*=1.5)		OM - (*M*=2)	
	η^{CMOD} (±0.05)	η^{FLD} (±0.40)	η^{CMOD} (±0.06)	η^{FLD} (±0.51)	η^{CMOD} (±0.08)	η^{FLD} (±0.25)	η^{CMOD} (±0.09)	η^{FLD} (±0.22)
0.10	1.00	0.80	1.06	1.22	0.93	0.35	0.86	0.16
0.20	1.00	1.24	1.06	1.65	0.93	0.83	0.86	0.64
0.30	1.00	1.68	1.06	2.09	0.93	1.31	0.86	1.11
0.40	1.00	2.11	1.06	2.53	0.93	1.79	0.86	1.59
0.50	1.00	2.55	1.06	2.97	0.93	2.26	0.86	2.07
0.60	1.00	2.55	1.06	2.78	0.93	2.26	0.86	2.07
0.70	1.00	2.55	1.06	2.60	0.93	2.26	0.86	2.07
a/W	SEN(B) base		UM - (*M*=0.5)		OM - (*M*=1.5)		OM - (*M*=2)	
	η^{CMOD} (±0.07)	η^{FLD} (±0.20)	η^{CMOD} (±0.05)	η^{FLD} (±0.36)	η^{CMOD} (±0.04)	η^{FLD} (±0.35)	η^{CMOD} (±0.05)	η^{FLD} (±0.21)
0.10	1.08	1.00	1.13	1.13	1.01	0.89	0.97	0.75
0.20	0.86	1.32	0.90	1.45	0.80	1.21	0.75	1.07
0.30	0.80	1.63	0.84	1.76	0.75	1.52	0.69	1.38
0.40	0.75	1.95	0.79	2.08	0.70	1.84	0.64	1.70
0.50	0.70	1.95	0.74	2.08	0.64	1.84	0.59	1.70
0.60	0.65	1.95	0.69	2.08	0.59	1.84	0.54	1.70
0.70	0.59	1.95	0.63	2.08	0.54	1.84	0.48	1.70
a/W	DEN(T) base		UM - (*M*=0.5)		OM - (*M*=1.5)		OM - (*M*=2)	
	η^{CMOD} (±0.15)	η^{FLD} (±0.23)	η^{CMOD} (±0.08)	η^{FLD} (±0.25)	η^{CMOD} (±0.20)	η^{FLD} (±0.21)	η^{CMOD} (±0.12)	η^{FLD} (±0.11)
0.20	0.81	0.38	0.95	0.59	0.75	0.22	0.67	0.12
0.30	0.81	0.44	0.95	0.65	0.71	0.27	0.63	0.18
0.40	0.81	0.49	0.95	0.70	0.67	0.33	0.59	0.23
0.50	0.81	0.54	0.95	0.76	0.63	0.38	0.55	0.29
0.60	0.81	0.60	0.95	0.81	0.58	0.44	0.51	0.34
0.70	0.81	0.65	0.95	0.87	0.54	0.49	0.47	0.40
a/W	M(T) base		UM - (*M*=0.5)		OM - (*M*=1.5)		OM - (*M*=2)	
	η^{CMOD} (±0.07)	η^{FLD} (±0.30)	η^{CMOD} (±0.14)	η^{FLD} (±0.25)	η^{CMOD} (±0.11)	η^{FLD} (±0.45)	η^{CMOD} (±0.09)	η^{FLD} (±0.20)
0.20	0.95	0.55	1.13	1.08	0.79	0.25	0.73	0.04
0.30	0.93	0.62	1.11	1.08	0.78	0.35	0.71	0.16
0.40	0.92	0.68	1.10	1.08	0.77	0.45	0.70	0.27
0.50	0.91	0.75	1.09	1.08	0.76	0.55	0.69	0.39
0.60	0.90	0.81	1.08	1.08	0.74	0.65	0.68	0.51
0.70	0.89	0.88	1.06	1.08	0.73	0.74	0.66	0.62

scatter specified, are independent to hardening exponents *N*, weld width ratio *h/W* and plane/stress/strain state *P*ε, *P*σ, within the bounds specified. The correlations are based on the assumption that the mechanical properties of welds and base material will differ producing weld under and over match mismatch factors between 0.5 and 2.0 (**66, 67**). For geometries in Table A2.1 the user must determine the welds strength factor before choosing the correct lower or upper bound values for η^{CMOD} and η^{FLD} in Tables A3.1 and A3.2. However, as an estimate, for the geometries in Fig. A1.3, the values of ±25% above and below the base material for all the geometries may be adopted for weld specimens depending on the level of weld miss-match.

TABLE A3.2 Summary of Best Fit Equations Relating the Sensitivity of the Mean Values of M to η in Six Fracture Specimens Giving the Upper/Lower Bound Variation Range Within the Crack Lengths Specified (67)

C(T):	$\eta^{LLD} = 2.71 - 0.38M \pm 0.20$	$0.45 \le a/W \le 0.7$
CS(T):	$\eta^{CMOD} = 4.27 - 0.49M \pm 0.38$	$0.3 \le a/W \le 0.7$
	$\eta^{LLD} = 2.50 - 0.29M \pm 0.12$	$0.3 \le a/W \le 0.7$
SEN(T):	$\eta^{CMOD} = 1.13 - 0.13M \pm 0.09$	$0.1 \le a/W \le 0.7$
	$\eta^{LLD} = 3.03 - 0.49M \pm 0.22$	$0.5 \le a/W \le 0.7$
SEN(B):	$\eta^{CMOD} = 0.79 - 0.08M \pm 0.12$	$0.2 \le a/W \le 0.7$
	$\eta^{LLD} = 2.21 - 0.25M \pm 0.14$	$0.4 \le a/W \le 0.7$
DEN(T):	$\eta^{CMOD} = 1.05 - 0.24M \pm 0.16$	$0.3 \le a/W \le 0.7$
	$\eta^{LLD} = 1.06 - 0.34M \pm 0.18$	$0.5 \le a/W \le 0.7$
M(T):	$\eta^{CMOD} = 1.29 - 0.26M \pm 0.14$	$0.2 \le a/W \le 0.7$
	$\eta^{LLD} = 1.35 - 0.38M \pm 0.15$	$0.2 \le a/W \le 0.7$

A4. GUIDELINES FOR USE OF ELECTRIC POTENTIAL DIFFERENCE (PD) FOR CRACK SIZE DETECTION

A4.1 *Voltage versus Crack Size Relationships for all the Specimens*—The initial and final potential difference (PD) readings correspond to the initial and final crack sizes, respectively, during the test. For the intermediate points, crack size at any instant may be determined by a direct linear interpolation of the PD data corresponding to the measured initial crack size, a_o, and final measured crack size, a_f, provided both a_o and a_f can be precisely measured on the fracture surface of the specimen at the end of the test. Thus, the crack size at any instant, a is given by:

$$a = \left[(a_f - a_o) \frac{(V - V_o)}{(V_f - V_o)} \right] + a_o \qquad \text{(A4.1)}$$

where:

V_o and V_f = initial and final potential difference readings, respectively, and
V = instantaneous potential difference corresponding to the crack size, a.

A4.2 If a_f was unavailable it is recommended to use $a_f = 0.75$ a/W and follow the calculations in Annex A4. However method may give an overestimate of the cracking rate and a repeat test should be made to confirm the results.

A4.3 If potential drop was unavailable the simple approximation of the initial to final crack size divided by the total time will give an approximate value for da/dt. A repeat test may be needed to confirm the results.

A4.4 For the C(T) specimen a predetermined relationship between measured voltage and crack size suitable for the chosen specimen geometry and input and output lead locations may be used to determine crack size as a function of time. For example, for an input current and voltage lead locations at the back face of the specimen shown in Fig. A1.5, the following closed form equation can be used to compute crack size from measured V/V_o values (**53**):

$$a/W = \frac{2}{\pi} \cos^{-1} \left[\frac{\cosh(\pi\ Y_o/2W)}{\cosh\left[\frac{V}{V_o} \cosh^{-1} \left\{ \frac{\cosh \pi\ Y_o/2W}{\cos \pi\ a_o/2W} \right\} \right]} \right] \qquad \text{(A4.2)}$$

where:

a_o = reference crack size with respect to the reference voltage, V_o. Usually, a_o will be initial crack size, a_o and V_o is the initial voltage,
Y_o = half distance between the output voltage leads, and
V = output voltage.

NOTE A4.1—Eq A4.2 may also be used to estimate crack size as a function of time if the measured value of a_f is not available. This may give a wrong prediction and therefore in such an instant it is recommended that additional test be performed to validate the data obtained on this specimen using the above method.

A4.5 If validity criteria are met and a final crack size, a_f, is available, a correction of all data between a_o and a_f is recommended by linear interpolation as given by:

$$a = \left[\frac{(a_f - a_o)}{(a_{pf} - a_o)} (a_p - a_o) \right] + (a_o) \qquad \text{(A4.3)}$$

where:

a_{pf} = final predicted crack size,
a_f = actual crack size, and
a_o = initial crack size.

A4.6 *Measurement of Thermal Voltage for Direct Current Technique*—The voltages V and V_o used for determining crack size in the equation in A4.1 may be different from their respective indicated readings when using a direct current technique. This difference is caused by the thermal voltage, V_{th}, caused by the minor differences in the junction properties or the resistances of the two output leads. An initial measurement of V_{th} is necessary. This can be accomplished by shutting off the current and recording the output voltage. In addition to the initial measurement, a periodic measurement of V_{th} also should be made by shutting off the current for short periods of time during testing. The values of V_{th} must be subtracted from the indicated values of V and V_o before substituting them in the equation given in A4.4.

NOTE A4.2—The guidelines for use of electric potential difference for crack size determination outlined in the Annex of Test Method E647 are applicable in their entirety for creep crack growth measurements also. The readers should consult this test method for recommendations on how to use this technique.

A4.7 *Discussion*—It should be noted that in some cases the initial PD readings at the beginning of the tests could drop before stabilization and eventually increase with crack extension. Conditions of initial loading, plasticity, excessive creep and damage and crack tip oxidation could affect the extent of this drop in the PD. In such cases, it is recommended that the minimum value of PD attained should be extrapolated back to zero time before crack size determinations are made. There is likelihood of increased scatter in crack size measurements during initial periods of testing.

APPENDIXES

(Nonmandatory Information)

X1. RECOMMENDED DATA REDUCTION TECHNIQUES

X1.1 *Secant Method*:

X1.1.1 The secant or point-to-point technique for computing crack growth rate and deflection rate simply involves calculating the slope of a straight line connecting two adjacent data points on the a versus t and the V versus t curve. It is formally expressed as follows:

$$\left(\frac{da}{dt}\right)_{\bar{a}} = (a_{i+1} - a_i)/(t_{i+1} - t_i) \tag{X1.1}$$

$$\left(\frac{dV}{dt}\right)_{\bar{a}} = (V_{i+1} - V_i)/(t_{i+1} - t_i) \tag{X1.2}$$

X1.1.2 Since the computed da/dt and dV/dt are average rate over the $(a_{I+1} - a_i)$ increment, the average crack length, $\bar{a} = ½\,(a_{i+1} + a_i)$, is normally used to calculate K, J, $C^*(t)$ and C_t.

X1.2 *Incremental Polynomial Method*:

X1.2.1 This method for computing da/dt, and dV/dt involves fitting a second order polynomial (parabola) to sets of $(2n + 1)$ successive data points, where n is commonly 3.

X1.2.2 The form of the equation for the local fits is as follows:

$$\hat{a}_i = b_{01} + b_{11}\left(\frac{t_i - C_1}{C_2}\right) + b_{21}\left(\frac{t_i - C_1}{C_2}\right)^2 \tag{X1.3}$$

$$\hat{V}_i = b_{02} + b_{12}\left(\frac{t_i - C_1}{C_2}\right) + b_{22}\left(\frac{t_i - C_1}{C_2}\right)^2 \tag{X1.4}$$

where:

$$-1 \le \left(\frac{t_i - C_1}{C_2}\right) \le +1$$

b_{01}, b_{11}, b_{21}, b_{02}, b_{12}, and b_{22} are regression parameters that are determined by the least squares method (that is minimization of the square of the deviations between observed and fitted values of crack length and deflection) over the range respectively. The values a_i and V_i are the fitted values of crack length and deflection at t_i. The parameters $C_1 = 0.5\ (t_{i-n} + t_{i+n})$ and $C_2 = 0.5\ (t_{i-n} - t_{i+n})$ are used to scale input data, thus avoiding numerical difficulties in determining the regression parameters. The rates of crack growth and increase in deflection at t_i are obtained from the derivatives of the Eq X1.5 and X1.6 and are given by the following expressions:

$$(da/dt)\hat{a}_i = b_{11}/C_2 + 2b_{21}(t_i - C_1)/C_2^2 \tag{X1.5}$$

and:

$$(dV/dt)\hat{V}_i = b_{12}/C_2 + 2b_{22}(t_i - C_1)/C_2^2 \tag{X1.6}$$

X1.2.2.1 The values of K, J, $C^*(t)$ and C_t associated with the above rates are computed using the fitted crack length, $\hat{a}_i$, corresponding to t_i.

X2. INCLUDING PLASTICITY IN ESTIMATION OF CREEP DEFLECTION RATE

X2.1 It is assumed that the mechanism for sub-critical creep crack-growth render it as basically a stationary crack. On this basis, J solutions for stationary cracks are valid for use. Furthermore the plasticity due to force-up, in addition to initial creep, both contribute to accelerate crack tip relaxation and allow a faster time for crack tip damage to develop and the cracks to grow. Therefore in the presence of significant plastic deformation, the deflection rate due to creep and plasticity may be estimated using the following equations (**36**):

$$\dot{V}_c = \dot{V} - \frac{\dot{a} B_N}{P}\left(\frac{2K^2}{E'} + (m+1)J_p\right) \tag{X2.1}$$

where:

J_p = fully-plastic contributions to J-integral, and
m = stress exponent in the Ramberg-Osgood stress versus strain relationship ($\varepsilon_p = D_1(\sigma/\sigma_{ys})^m$), where, D_1 = constant.

X2.2 Calculate the plastic contribution to J, J_p as follows for C_t specimens (**63**):

$$J_p = \frac{D_1 h_1(a/W, m)}{(\sigma_{ys}(W-a))^m}\left(\frac{P}{1.455\, B_N \alpha}\right)^{m+1} \tag{X2.2}$$

where:

$\alpha = (\varphi^2 + 2\varphi + 2)^{1/2} - (\varphi + 1)$, and
$\varphi = \frac{2_a}{(W-a)}$

X2.2.1 D_1 and m are constants that relate to the material's stress-strain behavior and h_1 is a function of a/W and m and is given in Table X2.1. The plane strain values are listed as they are conservative and also the criteria for stable creep crack growth constitute conditions that need higher constraint as the crack tip (see 11.8.5).

TABLE X2.1 h_1 (a/W, m) Values for C(T) Specimens Under Plane Strain Conditions (63)

a/W	h_1								
	m = 1	2	3	5	7	10	13	16	20
0.25	2.23	2.05	1.78	1.48	1.33	1.26	1.25	1.32	1.57
0.375	2.15	1.72	1.39	0.970	0.693	0.443	0.276	0.176	0.098
0.50	1.94	1.51	1.24	0.919	0.685	0.461	0.314	0.216	0.132
0.625	1.76	1.45	1.24	0.974	0.752	0.602	0.459	0.347	0.248
0.75	1.71	1.42	1.26	1.033	0.864	0.717	0.575	0.448	0.345
1	1.57	1.45	1.35	1.18	1.08	0.950	0.850	0.730	0.630

REFERENCES

(1) Rice, J. R., "A Path Independent Integral and the Approximate Analysis of Strain Concentration by Notches and Cracks. Journal of Applied Mechanics," *Transactions of the ASME*, 1968, pp. 379-386.

(2) Landes, J. D., and Begley, J. A., "A Fracture Mechanics Approach to Creep Crack Growth," *Mechanics of Crack Growth, ASTM STP 590*, ASTM, 1976, pp. 128-148.

(3) Nikbin, K. M., Webster, G. A., and Turner, C. E., "Relevance of Nonlinear Fracture Mechanics to Creep Cracking," *Crack and Fracture, ASTM STP 601*, ASTM, 1976, pp. 47-62.

(4) Saxena, A., "Evaluation of C* for the Characterization of Creep Crack Growth Behavior in 304 Stainless Steel," *Fracture Mechanics: Twelfth Conference, 1980 ASTM STP 700*, ASTM, pp. 131-151.

(5) Saxena, A., "Creep Crack Growth under Non Steady-State Conditions," *Fracture Mechanics: Seventeenth Volume, ASTM STP 905*, ASTM, Philadelphia, 1986, pp. 185-201.

(6) Ohji, K., Ogura, K and Kubo, S., *Jpn. Soc. Mech. Engng*. 44, 1975, pp. 1831-1838.

(7) Taira, S., Ohtani, R. and Kitamura, T., "Application of j-Integral to high-temperature crack growth propagation," trans. of *ASME J.Eng. Mater. Technol*., 101, 1979, pp. 154-167.

(8) Koterazawa, R., Mori, T., "Applicability of fracture mechanics parameters to crack propagation under creep conditions," Trans. of *AME J. Eng. Technol*., 99, 1977, pp. 298-305.

(9) Hui, C. Y., "Steady-State Crack Growth in Elastic Power Law Creeping Materials," *Elastic-Plastic Fracture, Vol. 1, ASTM STP 803*, ASTM, Philadelphia, 1983, pp. 573-593.

(10) Riedel, H., and Rice, J. R., "Tensile Cracks in Creeping Solids," *Fracture Mechanics: Twelfth Conference, ASTM STP 700*, ASTM, 1980, pp. 112-130.

(11) Gibbons, T. B., Guest editor, "Creep Crack Growth," a special issue of *Materials at High Temperatures*, Vol 10, No. 2, May 1992.

(12) Webster, G. A., and Ainsworth R. A., *High Temperature Components Life Assessment* , Chapman and Hall, London, 1994.

(13) Saxena, A., *Nonlinear Fracture Mechanics for Engineers*, CRC Press, Boca Raton, F1, 1998.

(14) Saxena, A., Hall, D. E., and McDowell, D. L., "Assessment of Deflection Rate Partitioning for Analyzing Creep Crack Growth Rate Data," *Engineering Fracture Mechanics*, Vol 62, 1999, pp 111-112.

(15) Bassani, J. L., Hawk, D. E., and Saxena, A., "Evaluation of the Ct Parameter for Characterizing Creep Crack Growth Rate in the Transient Regime," *Nonlinear Fracture Mechanics: Time-Dependent Fracture Mechanics*, Vol I, ASTM STP 995, ASTM, Philadelphia, 1989, pp. 7-29.

(16) Adefris, N. B., McDowell, D, L., and Saxena, A., "An Alternative Analytical Approximation of the Ct Parameter," *Fatigue and Fracture of Engineering Materials and Structures*, Vol 21, 1998, pp. 375-386.

(17) Nikbin, K. M., Smith, D. J., and Webster, G. A., "An Engineering Approach to the Prediction of Creep Crack Growth," *Journal of Engineering Materials and Technology*, Trans. ASME, Vol 108, 1986, pp. 186-191.

(18) Saxena, A., Han, J., and Banerji, K., "Creep Crack Growth Behavior in Power Plant Boiler and Steam Pipe Steel," *Journal of Pressure Vessel Technology*, Vol 110, May 1988, pp. 137-146.

(19) Liaw, P. K., Saxena, A., and Schaffer, J., "Estimating Remaining Life of Elevated-Temperature Steam Pipes—Part II. Fracture Mechanics Analysis," *Engineering Fracture Mechanics*, Vol 32, No. 5, 1989, pp. 769-722.

(20) Nikbin, K. M., Smith, D. J., and Webster, G. A., "Prediction of Creep Crack Growth from Uniaxial Creep Data," *Proc. Roy. Soc*. A.396, 1984, pp. 183-197.

(21) Nikbin, K. M., Smith, D. J., and Webster, G. A., "An Engineering Approach to the Prediction of Creep Crack Growth," *J. Eng. Mat. and Tech*., Trans ASME, 108, 1986, pp. 186-191.

(22) Yatomi, M., Nikbin, K. M., O'Dowd, N. P., and Webster, G, "Theoretical and Numerical Modelling of Creep Crack Growth in a Carbon-Manganese Steel," submitted, *Eng. Fract. Mechanics*, May 2005.

(23) API RP 579, "Standardized Fitness-for-Service Assessment Techniques for Pressurized Equipment Used in the Petroleum Industry," API, 2004.

(24) ASME Boiler and Pressure Vessel Code, Section XI, Division 1, "Rules for In-Service Inspection of Power Plant Components," ASME, 2001.

(25) AFCEN "Design and Construction Rules for Mechanical Components of FBR Nuclear Islands," RCC-MR, Appendix 16, "Guide for Defect Assessment and Leak Before Break Analyses," AFCEN, Paris, 2002.

(26) R5 "Assessment Procedure for the High Temperature Response of Structures Containing Defects," Issue 2, British Energy Generation Ltd, 2001.

(27) R6 "Assessment of the Integrity of Structures Containing Defects," Revision 3, British Energy Generation Ltd, 2000.

(28) BS 7910:1999 "Guide on Methods for Assessing the Acceptability of Flaws in Fusion Welded Structures," BSI, London, 1999.

(29) Schwalbe, K. H., Ainsworth, R. H., Saxena, A., and Yokobori, T., "Recommendations for Modifications of ASTM E1457 to Include Creep-Brittle Materials," *Engineering Fracture Mechanics*, Vol 62, 1999, pp. 123-142.

(30) Saxena, A., and Yokobori, T., editors, "Crack Growth in Creep-Brittle Materials," special issue of *Engineering Fracture Mechanics*, Vol 62, No. 1, 1999.

(31) Ainsworth, R. A., *Fatigue and Fracture of Engineering Materials and Structures*, Vol 10, 1987, pp. 115-127.

(32) Hall, D. E., McDowell, D. L., and Saxena, A., "Crack Tip Parameters for Creep-Brittle Crack Growth," *Fatigue and Fracture of Engineering Materials and Structures*, Vol 21, 1998, pp. 387-402.

(33) Hamilton, B. C., and Saxena, A., "Transient Crack Growth Behavior in Aluminum Alloys C415-T8 and 2519-T87," *Engineering Fracture Mechanics*, Vol 62, 1999, pp. 1-22.

(34) Tabuchi, M., Kubo, K., Yagi, K., Yokobori, A. T., and Fuji, A., "Results of the Japanese Round-Robin on Creep Crack Growth Evaluation Methods for Ni-Base Superalloys," *Engineering Fracture Mechanics*, Vol 62, 1999, pp. 47-60.

(35) Kwon, O., Nikbin, K. M., Webster, G. A., and Jata, K. V., "Crack Growth in the Presence of Limited Creep Deformation," *Engineering Fracture Mechanics*, Vol 62, 1999, pp. 33-46.

(36) Saxena, A., and Landes, J. D., "Characterization of Creep Crack Growth in Metals," in *Advances in Fracture Research, Sixth International Conference on Fracture*, Pergammon Press, 1984, pp. 3977-3988.

(37) Bassani, J. L., Hawk, D. E. and Saxena, A., "Evaluation of the Ct Parameter for Characterizing Creep Crack Growth Rate in the Transient Regime," *Nonlinear Fracture Mechanics: Time-Dependent Fracture Mechanics, Vol I, ASTM STP 995*, ASTM, Philadelphia, 1989, pp. 7-29.

(38) Fuji A., Tabuchi M., Yokobori A. T., and Yokobori T., *Engineering Fracture Mechanics*, Vol 62, 1999, pp. 23-32; Saxena, A., "Evaluation of Crack Tip Parameters for Characterizing Crack Growth: Results of the ASTM Round-Robin Program," *Materials at High Temperatures*, Vol 10, 1992, pp. 79-91.

(39) Dogan, B., and Schwalbe, K. H., "Creep Crack Growth Behaviour of Ti-6242," *ASTM Symposium Proc., ASTM STP 1131*, Ernst, H. A., Saxena, A., and McDowell, D. L., Eds., Philadelphia, PA, 1992, pp. 284-296.

(40) Saxena, A., Dogan, B., and Schwalbe, K. H., "Evaluation of the Relationship between C^*, δ_5 and δ_t During Creep Crack Growth," *Proc. ASTM 24th Symp. on Fracture Mechanics, ASTM-STP 1207*, 1994, pp. 510-526.

(41) Yokobori, Jr. A.T., Shibata, M., Tabuchi, M., and Fuji, A., *Materials at High Temperatures*, Vol 15, 1998, pp. 65-62.

(42) Nikbin, K. M., Invited Editor, "Creep Crack Growth In Components," *International Journal of Pressure Vessels and Piping*, Elsevier Ltd., Vol 80, Issues 7-8, July-August 2003, pp. 415 -595.

(43) Link, R., and Nikbin, K. M., Chief Editors, "Fracture and Fatigue of Structures," *ASTM STP 1480, Journal of ASTM International*, 3(2), 2006 , Available online at www.astm.org

(44) Nikbin, K. M., "Influence of Residual Stress on Creep Crack Growth," *ASME, PVP Conf.*, Atlanta, GA, Aug. 2001.

(45) Davies, C. M., Mueller, F., Nikbin, K. M., O'Dowd, N. P., and Webster, G. A., "Analysis of Creep Crack Initiation and Growth in Different Geometries for 316H and Carbon Manganese Steels," *ASTM STP 1480, Journal of ASTM International*, 3(2), 2006, DOI: 10.1520/JAI13223. Available online at www.astm.org

(46) Davies, C. M., Kourmpetis, M., O'Dowd, N. P., and Nikbin, K. M., "Experimental Evaluation of the J or C^* Parameter for a Range of Cracked Geometries," *ASTM STP 1480, Journal of ASTM International*, 3(5), 2006 , DOI: 10.1520/JAI13220. Available online at www.astm.org

(47) Dogan, B., Ceyhan, U., Nikbin, K. M., Petrovski, B., and Dean, D. W., "European Code of Practice for Creep Crack Initiation and Growth Testing of Industrially Relevant Specimens," *ASTM STP 1480, Journal of ASTM International*, February 2006, Vol 3, No. 2, Paper ID JAI13223. Available online at www.astm.org

(48) Bucci, R. J., "Effect of Residual Stress on Fatigue Crack Growth Rate Measurement," *Fracture Mechanics: Thirteenth Conference ASTM STP 743*, American Society for Testing and Materials, 1981, pp. 28-47.

(49) Davies, C. M., Dean, D. W., Nikbin, K. M., and O'Dowd, N. P., "Interpretation of Creep Crack Initiation and Growth Data for Weldments," *Engineering Fracture Mechanics*, 2006, DOI: 10.1016/j.engfracmech.2006.08.010.

(50) Dogan, B., Nikbin, K. M., Petrovski, B., Ceyhan, U., and Dean, D. W., "Code of Practice for High Temperature Testing of Weldments," *Int. J. Pressure Vessels and Piping*, Vol 83, 2006, pp. 784-797.

(51) Wasmer, K., Nikbin, K. M., and Webster, G. A., "A Sensitivity Study of Creep Crack Growth in Pipes," *PVP*, Vol 438, "New and Emerging Computational Methods: Applications to Fracture, Damage and Reliability," pp. 17-24, ASME, New York, NY, 2002.

(52) Yatomi, M., Nikbin, K. M., "Sensitivity Analysis of Creep Crack Growth Prediction using The Statistical Distribution of Uniaxial Data," to be published in the *J. Eng. Failure Analysis*, Jan., 2005.

(53) Johnson, H. H., *Materials Research and Standard*, Vol 5, No. 9, 1965, pp. 442-445.

(54) Schwalbe, K. H., and Hellman, D., *Journal of Testing and Evaluation*, Vol 9, No. 3, 1981, pp. 218-221.

(55) Baker, J., O'Donnell, M. P., and Dean, D. W., "Use of the R5 Volume 4/5 Procedures to Assess Creep-Fatigue Crack Growth in a 316L (N) Cracked Plate at 650°C," Vol 8-9, July, 2003.

(56) Davies, C. M., O'Dowd, N. P., Dean D. W., Nikbin, K. M., and Ainsworth, R. A., "Failure Assessment Diagram Analysis of Creep Crack Initiation in 316H Stainless Steel," Vol- 8-9, July, 2003.

(57) Yokobori, Jr., A. T., Uesugi, T., Yokobori, T., Fuji, A., Kitagawa, M., Yamaya, I., Tabuchi, M., and Yagi, K., "Estimation of Creep Crack Growth Rate in IN100 based on the Q^* Parameter Concept," *J. of Mat. Science*, 33, 1998, pp. 1555-1562.

(58) Srawley, J. E., "Wide Range Stress Intensity Factor Expressions for ASTM 399 Standard Fracture Toughness Specimens," *Int. Journal of Fracture Mechanics*, Vol 12, 1976, pp. 475-476.

(59) Tada, H., Paris, P. C., and Irwin, G. R., *Stress Analysis of Cracks—Handbook* , ed. D.R. Co., St Louis, 1985.

(60) Kim, Y. J., Son, B. G., and Kim, Y. J., "Elastic-Plastic Finite Element Analysis for Double-Edge Cracked Tension (DE(T)) Plates," *Engineering Fracture Mechanics*, 71, 2004, pp. 945-966.

(61) Kim, Y. J., and Budden, P. J., "Plastic η-Factor Solutions of Homogeneous and Bi-Material SE(T) Specimens for Toughness and Creep Crack Growth Testing," *Fatigue and Fract.of Eng.Mat. and Struct.*, 24(11), 2001, pp. 751-760.

(62) Paris, P. C., Ernst, H., and Turner, C. E., *A J-Integral Approach to Development of η-Factors, in Fracture Mechanics: Twelfth Conference, ASTM STP 700*, American Society for Testing and Materials, 1980, pp. 338-351.

(63) Kumar, V., German, M. D., and Shih, C. F., "An Engineering Approach to Elastic-Plastic Fracture Analysis," *ERPI NP 1931*, Electric Power Research Institute, Palo Alto, CA, 1981.

(64) Yokobori Jr., A.T, Sugiura, A, Tabuchi, M , Yatomi, M , Kobayashi, K, and Nikbin, K , "Definition and estimation method of incubation time of creep crack growth for high Cr steels and their weldments (creep crack initiation)", *Strength, Fracture and Complexity* 7, 315–320 315, IOS Press, (2011/2012)DOI 10.3233/SFC-2012-0146.

(65) Davies, C. M., Hughes, D., Wimpory, R. C., Dean, D. W., and Nikbin, K. M. (2010, January 1), "Measurements of Residual Stresses In 316 Stainless Steel Weldments," in B. J. Wiersma, B. Bezensek, M. P. H. Brongers, F. W. Brust, B. Burdett, A. Chakraborty, X. K. Zhu (Eds.), *Proceedings Of The Asme Pressure Vessels And Piping Conference 2010*, Vol 6, PTS A AND B Bellevue, Wa: Amer Soc Mechanical Engineers 59, pp. 1265-1273.

(66) Zhou, H., Mehmanparast, A., Davies, C. M., and Nikbin, K. M., "Evaluation of Fracture Mechanics Parameters for Bi-Material Compact Tension Specimens," *Materials Research Innovations*, Vol 17, No. 5, 2013, pp. 318-322.

(67) Zhou, H., Biglari, F., Davies, C. M., Mehmanparast, A., and Nikbin, K. M., "Evaluation of Fracture Mechanics Parameters for a Range of Weldment Geometries with Different Mismatch Ratios," *Engng Fract Mech*, Vol. 124-125, July 2014, pp 30-51.